The dynamics of thioredoxin-dependent reactions

by

Mampolelo M. Photolo

BSc. (*Hons*) Genetics

Submitted in fulfillment of the academic requirements for the degree of Master of Science in the School of Life Sciences

University of KwaZulu-Natal

Pietermaritzburg

As the candidate's supervisor I have approved this dissertation for submission.

Signed: _____ Name: Dr C. S Pillay Date: _____

Preface

The experimental work described in this dissertation was carried out in the Discipline of Genetics, School of Life Sciences, University of KwaZulu-Natal, Pietermaritzburg, from February 2012 to May 2014 under the supervision of Dr C.S Pillay.

These studies represent original work by the author and have not otherwise been submitted in any form to another University. Where use has been made of the work by other authors it has been duly acknowledged in the text.

Name:

_____

Signed:

_____

Date:

_____

College of Science and Agriculture

Declaration of Plagiarism

I, Mampolelo M. Photolo declare that:

1. The research reported in this thesis, except where otherwise indicated, is my original research.
2. This thesis has not been submitted for any degree or examination at any other university.
3. This thesis does not contain other persons' data, pictures, graphs or other information, unless specifically acknowledged as being sourced from other persons.
4. This thesis does not contain other persons' writing, unless specifically acknowledged as being sourced from other researchers. Where other written sources have been quoted, then:
    a) Their words have been re-written but the general information attributed to them has been referenced
    b) Where their exact words have been used, then their writing has been placed in italics and inside quotation marks, and referenced.
5. This thesis does not contain text, graphics or tables copied and pasted from the Internet, unless specifically acknowledged, and the source being detailed in the thesis and in the References sections.

Signed:

_____

Date:

_____

Declaration Plagiarism 22/05/08 FHDR Approved

Table of Contents

Abstract

The thioredoxin system, comprising thioredoxin (Trx), thioredoxin reductase (TrxR) and NADPH, is present in most organisms from prokaryotes to eukaryotes. The system plays a central role in the redox regulation of several key cellular processes including DNA synthesis, apoptosis, glycolysis and redox signal transduction and changes in this system are associated with the progression of a number of diseases including certain cancers, malaria and HIV. Understanding the regulation of this network from a systems perspective is therefore essential. Our lab developed the first computational model of the *Escherichia coli* thioredoxin system and analyzed this system using mathematical and core models. In contrast to the commonly held assumption of the thioredoxin network as an electrical circuit with no cross-talk, our analysis showed this system displayed ultrasensitivity, adaptability and was interconnected via the thioredoxin redox cycle. In this study, a model of the *Saccharomyces cerevisiae* thioredoxin system was developed and computational modeling showed that an increase in concentration of one of the substrates in the thioredoxin system could decrease the flux of another thioredoxin oxidation reaction in a concentration-dependent manner. To complement these computational analyses, yeast thioredoxin reductase and thioredoxin were cloned, expressed and purified. An *in vitro* kinetic assay using insulin as a substrate and immunoglobin Y (IgY) as a competing substrate was subsequently undertaken. Our results showed that in some cases an increase in IgY concentration affected the rate of insulin reduction as measured by turbidity at 650 nm confirming the computational model's prediction. However, unexpectedly, with an increase in IgY concentration, there was a decrease in apparent absorbance at 650 nm at longer time points. These *in silico* and *in vitro* analyses shed light on how the thioredoxin system connects seemingly unrelated parts of metabolism into an integrated network, but additional experiments are required in order to improve the kinetic analyses in this study.

Acknowledgements

I would like to express my most genuine appreciation to the following people for all their assistance in to this thesis:

I would like to express my special appreciation and thanks to my supervisor Dr Ché Pillay, who has been a tremendous mentor for me. I would like to thank you for encouraging my research and for allowing me to grow as a research scientist. Your advice on my research and your understanding of the battles that life has thrown my way was really priceless. You have really been “coolish megoolish”

Dr. Gregory Watson for advice on all the molecular biology work.

Letrisha Padayache for generously sharing her *TRX1* clones with me and for giving me advice on all the drama I experienced (inside and outside the lab).

Lefentse Mashamaite and Scott Driscoll for being my super computational modeling gurus.

To my current and ex lab sisters, Lee, Tersh, Erasha, Melissa, Nicole, Beatrice and our special adoptee Mary. Thank you guys for keeping me sane half the time.

To Mary, Lee, Tersh and Smalls, thank you for Long Street, that night will never be forgotten.

The Conservation genetics lab and Megan for the use of equipment and Ntate Goodman Zondi for all his help.

Sanele Mnkandla and Jacky for protein work advice and lending me PEG in times of need.

To my late dad, to whom this thesis is dedicated to, my sweetheart, I wish you could be here to share these moments with me. You will never be forgotten.

My mommy, I don't know what I would do without you in my life. Thank you for being my rock and my pillar of strength. Thank you for always being optimistic and praying for me. I am very lucky to have a mother like you.

To my one and only awesome brother Matt, his wife Queen-Sabi, my crazy big sister, Mpho and my drama queen Nonoza, I am blessed to have you guys in my life, your support means a

lot to me. It is because of you guys that I have entertainers like DT, Rei2, Tshepi, Joss and Maketela to take a million pictures with.

Lindt, thank you for always being on my side and actually taking the time to understand what my research was about, although it may have sounded like Greek to you.

Phindile, you have kept me sane outside campus when things were just a drag in PMB for me. Thank you for offering me your couch and just being there every time I needed a friend.

Msizi, even though we could go for months without a hello, we always connect like we last met yesterday. Thank you for allowing me to vent about my research drama to you.

The National Research Foundation and the Faculty of Science and Agriculture for generous scholarships during my post-graduate years.

Most importantly I thank Jehova Modimo for the perseverance that He has bestowed upon me during this research project, and indeed, throughout my life: "I can do all things through Christ who strengthens me." (Philippians 4: 13)

List of abbreviations

APS	Ammonium persulphate
BSA	Bovine serum albumin
dH_2O	Distilled water
DTNB	5, 5'-dithiobis (2-nitrobenzoic acid)
DTT	Dithiothreitol
EDTA	Ethylene diamine tetraacetic acid
H_2O_2	Hydrogen peroxide
IPTG	Isopropyl β-D-1-thiogalactopyranoside
LB	Luria Bertani
NADPH	β-nicotinamide adenine dinucleotide phosphate
NTC	No template control
PCR	Polymerase Chain Reaction
PEG	Polyethylene glycol
PySCeS	Python Simulator of Cellular Systems
SDS-PAGE	Sodium dodecyl sulfate-polyacrylamide gel electrophoresis
TEMED	N,N,N',N'-tetramethylethylenediamine
Trx	Thioredoxin
YPD	Yeast peptone dextrose
SOC	Super Optimal broth
TE buffer	Tris-EDTA buffer
ECEF	Eosinophil cytotoxicity-enhancing factor
RNR	Ribonucleotide reductase

List of Tables

List of Figures

Chapter 1: LITERATURE REVIEW

1.1 Introduction

Cellular mechanisms that regulate redox homeostasis are vital as they provide a buffer against conditions that may disturb the redox environment of cells and induce oxidative stress (Schafer and Buettner, 2001; Perrone *et al*., 2008). The thioredoxin system is widely distributed among prokaryotes and eukaryotes, and plays a vital role in maintaining the redox homeostasis of the cell (Arnér and Holmgren, 2006). In this system, reducing equivalents are transferred from NADPH to thioredoxin by thioredoxin reductase (Fig. 1.1). Thioredoxin in turn reduces a large number of targets involved in several critical cell functions (Arnér and Holmgren, 2000a).

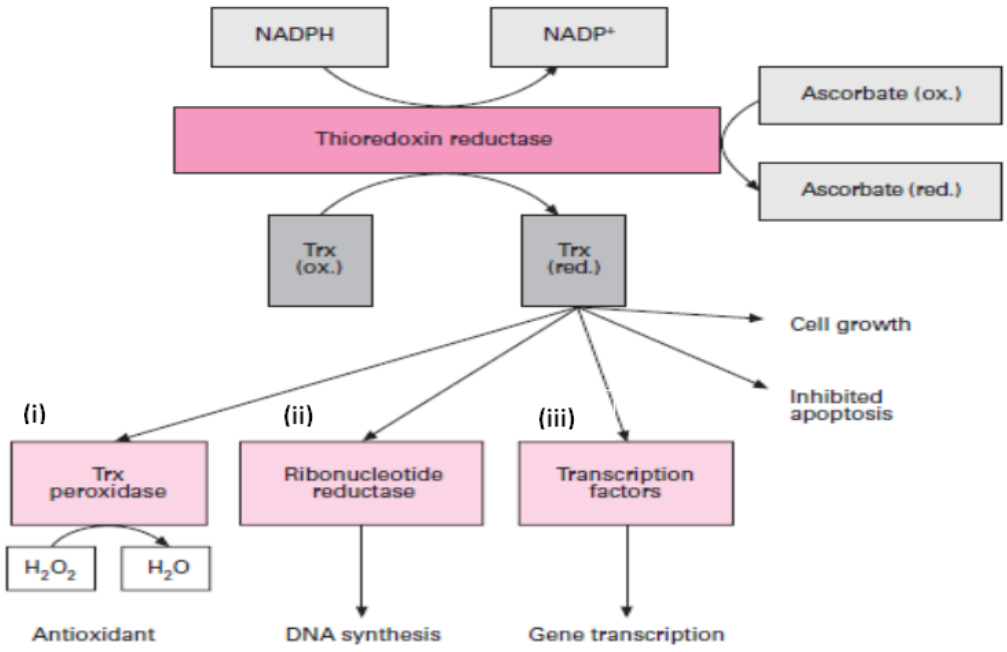

Figure 1.1 Diagrammatic representation of the reactions and functions of the thioredoxin system. Reduced thioredoxin provides reducing equivalents to (i) thioredoxin peroxidase, which breaks down H_2O_2 to water, (ii) ribonucleotide reductase, which reduces ribonucleotides to deoxyribonucleotides for DNA synthesis, and (iii) transcription factors, which leads to their increased binding to DNA and altered gene transcription (Mustacich and Powis, 2000).

This system was first discovered as an electron donor for the enzymatic synthesis of cytodine deoxyribonucleoside diphosphate by ribonucleotide reductase (RNR) from *Escherichia coli* (Laurent *et al*., 1964; Buchanan *et al.*, 2012). Subsequently, *E. coli* thioredoxin was isolated, sequenced and was found to contain the now classic active site, -

Cys-Gly-Pro-Cys- (Holmgren, 1968). *E. coli* thioredoxin reductase was also isolated and analysis of its kinetic properties showed that it was a specific reductant of thioredoxin (Moore *et al*., 1964).

The thioredoxin system is essential for maintaining the balance of the cellular redox status and is involved in the regulation of redox signalling. Moreover, it is crucial for growth promotion, neuroprotection, inflammatory modulation, antiapoptosis, immune function (Mahmood *et al*., 2013). As an ubiquitous and multifunctional protein, thioredoxin is expressed in all forms of life, executing its function through its antioxidative, protein-reducing, and signal-transducing activities (Lu and Holmgren, 2012). However, this system has been implicated in several human diseases such as cancer (Kim *et al*., 2003), malaria (Nickel *et al*., 2006), heart failure (Turoczi *et al*., 2003), neurodegenerative diseases (Lippoldt *et al*., 1995) and viral diseases such as human immunodeficiency virus (HIV) (Nakamura *et al*., 1996). Understanding the dynamics of this system using system biology approaches could be beneficial in the treatment of the above mentioned human diseases (D'Alessandro *et al*., 2011; Pillay *et al*., 2013).

1.2 The yeast thioredoxin system

The yeast, *Saccharomyces cerevisiae* contains a cytoplasmic thioredoxin system comprised of two thioredoxins (*TRX1*, *TRX2*) and a thioredoxin reductase (*TRR1*). Yeast also has a complete mitochondrial thioredoxin system comprised of the thioredoxin *TRX3* and the thioredoxin reductase *TRR2* which is thought to function in protection against oxidative stress generated during respiratory metabolism (Gan, 1991; Pedrajas *et al*., 1999). The cytoplasmic thioredoxins (*TRX1*, *TRX2*) and thioredoxin reductase (*TRR1*) are dispensable during normal growth conditions provided that a functional glutaredoxin/glutathione (Grx/GSH) system is present (Gan, 1991; Muller, 1991). These systems both belong to the thioredoxin superfamily whose members characteristically share the thioredoxin-fold.

Yeast also contains two genes encoding cytoplasmic glutaredoxins (*GRX1* and *GRX2*) which are also dispensable during normal growth provided that a functional thioredoxin system is present (Luikenhuis *et al*., 1997). The *S. cerevisiae* thioredoxin thiol redox system is therefore similar to that of *E. coli* as they both consist of the thioredoxin and glutathione/glutaredoxin pathways (Toledano *et al*., 2007) which are functionally overlapping (Trotter and Grant, 2002).

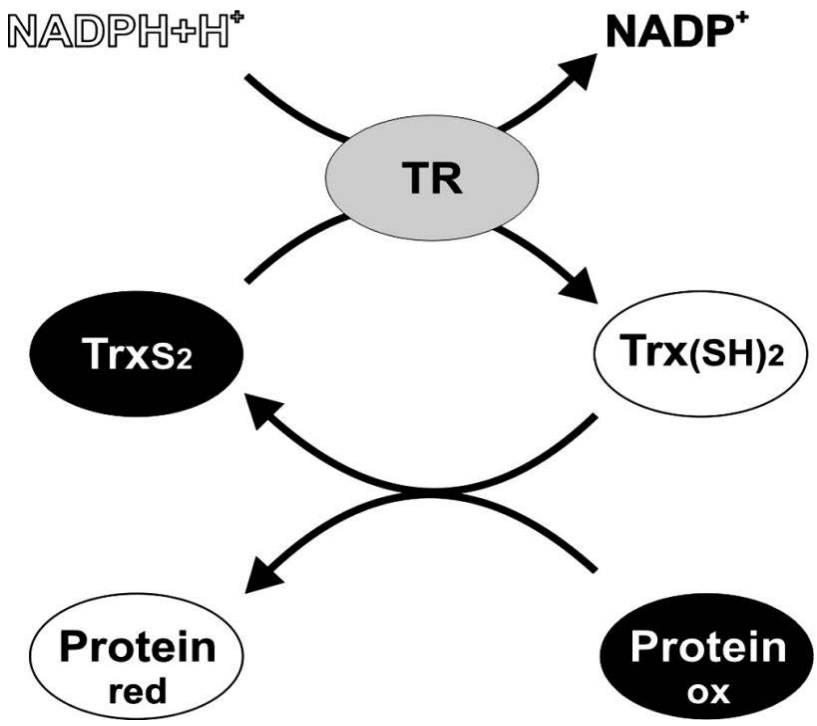

Figure 1.2 Diagrammatic representation of the thioredoxin system. Reduced thioredoxin ($Trx(SH)_2$) directly interacts with oxidized proteins (Protein ox) by reducing disulfide bridges. As a result, the target protein is reduced (Protein red) and thioredoxin itself is oxidized ($TrxS_2$). The regeneration of thioredoxin from its oxidized form is catalyzed by thioredoxin reductase (TR) using NADPH (Lukosz *et al*., 2010).

The first evidence that the thioredoxin and the glutathione/glutaredoxin systems share an overlapping function in redox regulation came from the identification of glutathione reductase (*GLR*) in a genetic screen for mutations which confer a requirement for thioredoxins (Muller, 1996). Furthermore, deletion analysis has shown that the quadruple yeast mutant (Δ*trx1*Δ*trx2*Δ*grx1*Δ*grx2*, Table 1.1) was not viable and a single functional disulphide reductase system is necessary for viability (Draculic *et al*., 2000). To further test the requirement for components of the thioredoxin and GSH systems, mutants lacking components of each system were constructed. Strains completely lacking the thioredoxin (Δ*trx1*Δ*trx2*Δ*trr1*) or glutathione (Δ*gsh1*Δ*glr1*) systems were viable, but strains simultaneously deleted for components of both systems (Δ*gsh1*Δ*trx1*Δ*trx2* and Δ*glr1*Δ*trr1*) were not viable. However, mutants lacking *TRX1* and *TRX2* (Δ*trx1*Δ*trx2*, Table 1.1) showed an increase in both oxidized GSSG and reduced GSH levels, together with an extended S-phase (Muller, 1996; Garrido and Grant, 2002). The extended S-phase was caused by a

decrease in the dNTP pools due to an absolute decrease of the RNR reduced form and an increase of its oxidized disulfide bond form (Muller, 1996). The extended S-phase indicated that GRX1 and GRX2 were not as efficient as TRX1 and TRX2 in RNR reduction (Muller, 1996). In summary, there is convincing evidence that these redox regulatory systems have many overlapping functions in terms of both regulation and substrate utilization. However in yeast, the thioredoxin system is more important in ribonucleotide reductase reduction. The properties of the individual components of the thioredoxin system will be described below.

Table 1.1 Phenotypes of thiol redox systems in *S. cerevisiae* (Toledano *et al*., 2007)

Mutant	Phenotype	Rescued by	Defects
Δ*trx1*	nl[a]		
Δ*trx2*	nl		
Δ*trr1*	Slow growth		
Δ*trx1*Δ*trx2*	Protracted S phase, Met auxotrophy	RNR overexpression	Sulfate assimilation, Ribonucleotide reduction
Δ*trr1*Δ*trx1*Δ*trx2*	Similar to Δ*trx1*Δ*trx2*	Similar to Δ*trx1*Δ*trx2*	Similar to Δ*trx1*Δ*trx2*
Δ*glr1*	nl		Accumulates GSSG
Δ*grx1*Δ*grx2*	nl		
Δ*grx1*Δ*grx2*Δ*trx1*Δ*trx2*	Unviable		Ribonucleotide reduction
Δ*trx1*Δ*trx2*Δ*glr1*	Unviable aerobically	Anaerobic weak growth	Complex
Δ*trr1*Δ*glr1*	Unviable aerobically		Complex
Δ*trx1*Δ*trx2*Δ*gsh1*	Unviable aerobically	ND	Complex

nl: Normal vegetative growth

1.2.1 Thioredoxin reductase

Thioredoxin reductase is the only known enzyme to maintain thioredoxin in a reduced state (Holmgren, 1985). Thioredoxin reductase is a member of a family of pyridine nucleotide disulfide oxidoreductases and members of this family are flavoproteins that contain one redox-active disulfide, one tightly bound flavin adenine dinucleotide (FAD) and an NAPDH binding site per subunit (Fig. 1.3; Williams, 1992), which is similar in the prokaryotes (archaea and bacteria) and eukaryotes such as yeasts (Kuriyan *et al*., 1991). *S. cerevisiae TRR1* and *TRR2* share a sequence identity of 85% (Fig. 1.4) and they both have the structural characteristics of thioredoxin reductases from lower organisms (Zhang *et al*., 2009).

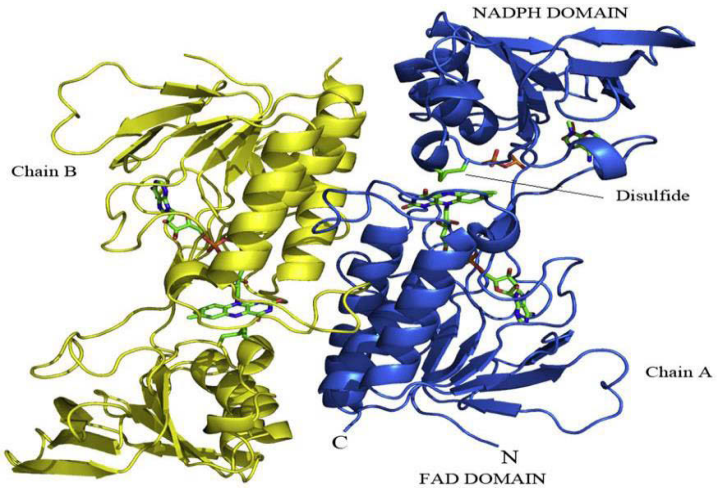

Figure 1.3 Structure of *Saccharomyces cerevisiae* thioredoxin reductase (*TRR1*) dimer. FAD molecules, adenine ring and three phosphate groups of NADPH and the disulfides of active sites were drawn using a ribbon model (Zhang *et al*., 2009).

Interestingly enough, activity assays indicated that Trr1 can also reduce *S. cerevisiae* thioredoxin-3 at a similar efficiency to that of Trr2 although they are located in different cellular compartments (Zhang *et al*., 2009). These results indicated that there was no selectivity within the *S. cerevisiae* thioredoxin system counterparts. This similar reductive efficiency was due to comparable k_{cat}^{app} values (Table 1.2; Oliveira *et al*., 2010).

```
Trr1  ----------------------MVHNKVTIIGSGPAAHTAAIYLARAEI 27
Trr2  MIKHIVSPFRTNFVGISKSVLSRMIHHKVTIIGSGPAAHTAAIYLARAEM 50
                           *:*:************************:

Trr1  KPILYEGMMANGIAAGGQLTTTTEIENFPGFPDGLTGSELMDRMREQSTK 77
Trr2  KPTLYEGMMANGIAAGGQLTTTTDIENFPGFPESLSGSELMERMRKQSAK 100
      ** ********************:********:.*:*****:***:**:*
Trr1  FGTEIITETVSKVDLSSKPFKLWTEFNEDAEPVTTDAIILATGASAKRMH 127
Trr2  FGTNIITETVSKVDLSSKPFRLWTEFNEDAEPVTTDAIILATGASAKRMH 150
      ***:******************:**********************************

Trr1  LPGEETYWQKGISACAVCDGAVPIFRNKPLAVIGGGDSACEEAQFLTKYG 177
Trr2  LPGEETYWQQGISACAVCDGAVPIFRNKPLAVIGGGDSACEEAEFLTKYA 200
      **********:**********************************:*****.

Trr1  SKVFMLVRKDHLRASTIMQKRAEKNEKIEILYNTVALEAKGDGKLLNALR 227
Trr2  SKVYILVRKDHFRASVIMQRRIEKNPNIIVLFNTVALEAKGDGKLLNMLR 250
      ***::*******:***.***:* *** :* :*:****************  **

Trr1  IKNTKKNEETDLPVSGLFYAIGHTPATKIVAGQVDTDEAGYIKTVPGSSL 277
Trr2  IKNTKSNVENDLEVNGLFYAIGHSPATDIVKGQVDEEETGYIKTVPGSSL 300
      *****.* *.** *.*********:***.** **** :*:***********

Trr1  TSVPGFFAAGDVQDSKYRQAITSAGSGCMAALDAEKYLTSLE 319
Trr2  TSVPGFFAAGDVQDSRYRQAVTSAGSGCIAALDAERYLSAQE 342
      ****************:*****:********:*******:**:: *
```

Figure 1.4 Alignment of the amino acid sequences of *S. cerevisiae* Trr1 and Trr2. The redox-sensitive motif is enclosed in a rectangle. Asterisks indicate identical residues. The sequence of Trr2 was used as reference for the identity/similarity values. Alignments were made using ClustalX.

Table 1.2 Comparison of kinetic parameters for the reduction of yeast thioredoxins by thioredoxin reductase 1 (Trr1) (Oliveira *et al*., 2010)

Substrate	K_M^{app} (μM)	k_{cat}^{app} (s^{-1})	k_{cat}/K_M^{app} ($1/\mu Ms^{-1}$)
Yeast thioredoxin-1-TRR1	1.3 ± 0.2	43.7 ± 2.5	$(3.4 \pm 1.2) \times 10^7$
Yeast thioredoxin-2-TRR1	0.6 ± 0.1	42.9 ± 1.5	$(7.3 \pm 1.5) \times 10^7$
Yeast thioredoxin-3-TRR1	1.1 ± 0.1	34.0 ± 1.1	$(3.1 \pm 1.1) \times 10^7$

1.2.2 Thioredoxin

Thioredoxin is a low molecular weight (12 kDa), thermostable protein and is present in all known living organisms (Holmgren, 1985). Thioredoxin can exist either in a reduced (thioredoxin-$(SH)_2$) or oxidized form (thioredoxin-S_2). The difference between these forms of thioredoxin involves a local conformational change in and around the redox-active disulfide (Arnér and Holmgren, 2000b).

The oxidised form of thioredoxin contains a single redox active disulfide that is formed from the two half-cystine residues of the protein. In the presence of thioredoxin reductase and NADPH, this disulfide is opened and the reduced form of thioredoxin is subsequently formed (Hall *et al*., 1971). This active form of thioredoxin becomes reoxidized while providing reducing equivalents to target molecules including ribonucleotide reductase, thioredoxin peroxidase and transcription factors (Fig. 1.1-1.2; Mustacich and Powis, 2000).

S. cerevisiae contains three thioredoxin isoforms. Thioredoxin-1 and thioredoxin-2 are cytosolic thioredoxin proteins and thioredoxin-3 is located in the mitochondria and is much larger than both thioredoxin-1 and thioredoxin-2 (Pedrajas *et al*., 1999). *TRX1* and *TRX2* share 78% amino acid identity, and 46% (*TRX1*) and 43% (*TRX2*) identity relative to *TRX3* (Fig. 1.5; Pedrajas *et al*., 1999).

The role of the thioredoxin system in certain disease pathogenesis states and the effect on the cellular redox balance in lung cancer and human immunodeficiency virus (HIV) are discussed below.

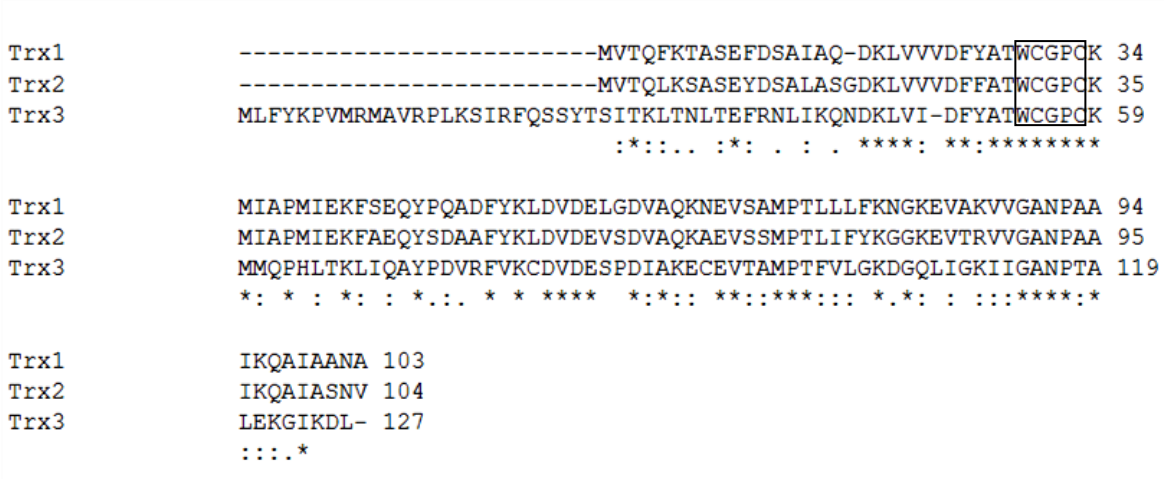

Figure 1.5 Alignment of the amino acid sequences of *S. cerevisiae* thioredoxin-1, thioredoxin-2, and thioredoxin-3. The redox active site is enclosed in a rectangle. Asterisks indicate identical residues. The sequence of thioredoxin-3 was used as reference for the identity/similarity values. Alignments were made using ClustalX (Pedrajas *et al*., 1999).

1.3 The thioredoxin system and disease

1.3.1 Cancer

Arnèr and Holmgren (2006) reviewed numerous scientific reports describing higher expression of thioredoxin and thioredoxin reductase in certain cancer tumors. For example, thioredoxin expression is increased in several primary cancers, including lung (Kim *et al*., 2003; Xu *et al*., 2012), cervix (Hedley *et al*., 2004), pancreatic (Han *et al*., 2002), colorectal (Raffel *et al*., 2003), hepatocellular carcinomas (Miyazaki *et al*., 1998), gastric carcinomas (Grogan *et al*., 2000) and breast cancer (Cha *et al*., 2009). Data also suggests that the high thioredoxin concentrations could be linked to resistance to chemotherapeutic agents including doxorubicin, cisplatin, docetataxel and tamoxifen (Karlenius and Tonissen, 2010). In one study for example, tumors with high thioredoxin expression showed a significantly lower response rate to docetaxel than those with low thioredoxin expression (Marks, 2006). In another study, gene expression profiling of 44 breast tumor samples treated with docetaxel and were analyzed. It was found that nearly half of the docetaxel resistant cells were characterized by elevated expression of redox genes, including glutathione S-transferase, peroxiredoxins and thioredoxin (Iwao-Koizumi *et al*., 2005). Furthermore, resistance of ovarian, gastric and colon cancer cells has been associated with increased intracellular thioredoxin levels (Marks, 2006; Yoshioka *et al*., 2006). These studies suggested that thioredoxin levels were elevated in many human primary cancers and this high expression

was associated with aggressive tumor growth and inhibited apoptosis (Karlenius and Tonissen, 2010).

1.3.2 Human Immunodeficiency Virus (HIV)

Elevated levels of the thioredoxin system have also been implicated and are indicative of oxidative stress during HIV infection (Pace and Leaf, 1995; Gromer *et al*., 2004). These elevated levels have been reported in the chronic stages of HIV-1 infection and may facilitate virus entry in macrophages (Stantchev *et al*., 2012). This was shown in a study where HIV-infected individuals had elevated levels of thioredoxin and displayed lower $CD4^+$ cell counts (Nakamura *et al*., 2001). These HIV-infected individuals showed increased plasma/serum levels of thioredoxin and patients with higher plasma thioredoxin die sooner than patients with normal plasma levels of thioredoxin (Nakamura *et al*., 2001; Van Laer *et al*., 2002). However, elevated levels of thioredoxin do not necessarily indicate advanced HIV-infection as thioredoxin levels were shown to have been elevated in some apparently healthy HIV-infected people (Nakamura *et al*., 1996).

In contrast to the serum levels, lymph node biopsies of HIV-patients showed a significant loss of thioredoxin-production in this tissue (Gromer *et al*., 2004). In addition, thioredoxin was also shown to be deficient in tissues from acquired immune deficiency syndrome (AIDS) patients (Nakamura *et al*., 1996). This may be explained by the ability of macrophages to convert thioredoxin into the C-terminally truncated 10 kDa protein called eosinophil cytotoxicity-enhancing factor (ECEF) (Fig. 1.6) which enhances HIV-production (Newman *et al*., 1994). Thus, whereas thioredoxin is a potent inhibitor of the expression of HIV in human macrophages, cleavage of thioredoxin to ECEF creates a mediator with the opposite effect (Newman *et al*., 1994).

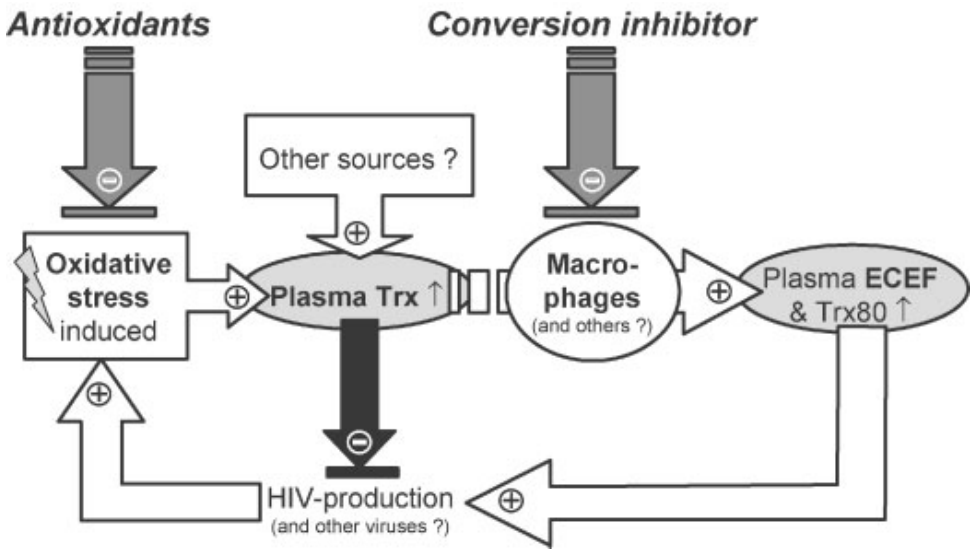

Figure 1.6 Schematic representation of the interaction of thioredoxin, ECEF and HIV-production. Indicated are theoretical therapeutic approaches. Trx80 is a 10 kDa truncated form of thioredoxin containing the 80 N-terminal residues. White arrows indicate stimulation and dark arrows indicate inhibition (Gromer *et al*., 2004).

1.3.3 Malaria

While changes in the human thioredoxin system are implicated in several diseases, a number of pathogens also rely on their thioredoxin systems to overcome oxidative stresses generated during host infection. These pathogens include *Plasmodium falciparum* (Holmgren and Lu, 2010) and *Trypanosomatid protozoa* (Krauth-Siegel and Comini, 2008).

P. falciparum, the protozoan parasite responsible for a million clinical malaria cases, is dependent on the antioxidant capacity of its host cell and its own peroxidases which both require the thioredoxin system to function (Nickel *et al*., 2006). Although the parasite possesses a glutathione peroxidase and a thioredoxin system, the host thioredoxin system is proposed to be the main detoxification system for reactive oxygen species (Adelekan *et al*., 1998). It has been demonstrated that the human redox protein peroxiredoxin-2 is imported from the host erythrocyte into the cytosol of *P. falciparum* in functional form and in significant concentrations (Koncarevic *et al*., 2009). This result provided insights into the interaction between malarial parasites and their host cells. Thus, instead of depleting its own resources, *P. falciparum* makes use of human peroxiredoxin-2 for its own survival (Koncarevic *et al*., 2009).

However, efforts at combating these above mentioned pathologies have been limited by the complexity of the thioredoxin system (Jones, 2010). As a result, analyzing the thioredoxin system and its regulation using a systems biology approach is required in order to acquire a clearer understanding of the integrated regulation and dynamics of the elements in this system (Kemp *et al*., 2008). This could be beneficial in the treatment of these pathologies in which redoxins are implicated.

1.4 Systems biology

The kinetics of individual thioredoxin-dependent reactions has been thoroughly studied. However, the kinetic regulation of the thioredoxin system as a whole is not yet known and there is not yet a complete theoretical frame work to base systems analysis on (Pillay *et al*., 2009). Although the thioredoxin system has an effect on several processes (Fig. 1.2), it was initially not clear whether thioredoxin-dependent reactions have an effect on each other and how the kinetic structures within the thioredoxin system contribute to the regulation of the system (Pillay *et al*., 2009). This question has been addressed by using kinetic modeling to identify and describe the kinetic behaviors found within the system (Pillay *et al*., 2011).

Two modeling approaches have since been developed to describe the behavior or activity of the thioredoxin system (Kemp *et al*., 2008; Pillay *et al*., 2011). In the first approach, thioredoxin is considered an enzyme and forms part of an electron circuit incorporating the major cellular redox couples (Kemp *et al*., 2008). The steady-state redox values for these couples are maintained separately for each couple by the balance of NADPH-dependent reduction and peroxide-dependent oxidation rates. This implies that each redox couple can be used for different redox-control processes independently (Kemp *et al*., 2008). The second model proposed that thioredoxins are redox couples and thioredoxin-dependent reactions affect each other through the thioredoxin redox cycle (Pillay *et al*., 2011). However, these results were obtained solely from computational analysis and it is not known whether the system displays this behaviour *in vitro* and *in vivo.*

The two different modelling approaches are shown below (Fig. 1.7). The one approach (*darker arrows on the left*) represents the electron flow modeling approach of the thioredoxin system (Kemp *et al*., 2008). In this approach, each couple is used for different redox-control processes (Kemp *et al*., 2008) with the reactions independent of one another, but are all dependent on the NADPH concentration. In contrast, the thioredoxin redoxin couple

approach focused on the kinetics of individual thioredoxin-dependent reactions in the system (Fig. 1.7; Pillay *et al*., 2011), with the thioredoxin reductase and individual thioredoxin reaction kinetic parameters affecting the connectivity within the system.

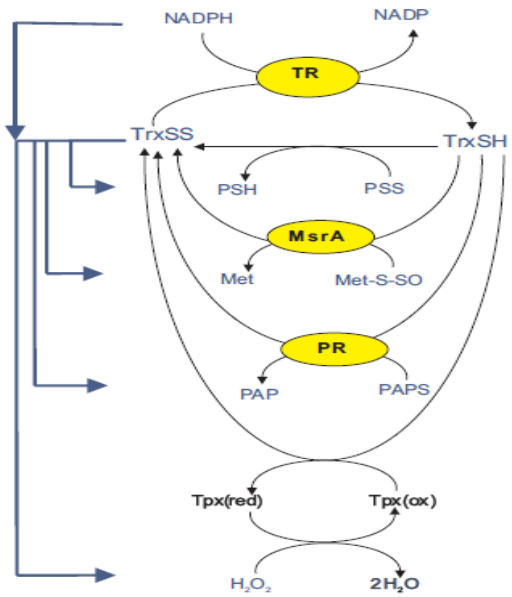

Figure 1.7 Modelling the thioredoxin system in *E. coli*. Shows reactions for reduction of oxidised thioredoxin (TrxSS) by thioredoxin reductase (TR), thioredoxin-dependent reductions of methionine sulfoxide (Met-S-SO) by methionine sulfoxide reductase (MsrA) and 3'-phosphoadenosine-5'-phosphosulfate (PAPS) by PAPS reductase and the Tpx-dependent reduction of hydrogen peroxide (Pillay *et al*., 2011).

1.5 Aims

Analyzing the dynamics of the thioredoxin system through the use of system biology approaches could prove to be useful for the quantification and understanding of the regulation of these systems in cells. An important step would be to distinguish between the redox couple and the electron flow models *in vitro*. However, there are limitations that need to be considered and addressed in order to complete these studies. Current activity assays require thioredoxin and thioredoxin reductase to be in a purified form. Therefore, yeast thioredoxin and thioredoxin reductase needed to be cloned, expressed and purified. In addition, we had to develop an assay to monitor the effect of two thioredoxin substrates on the dynamics of the system in order to distinguish between the redox couple and the electron flow models.

Chapter 2: GENERAL MATERIALS AND METHODS

General methods and materials that were regularly used throughout the duration of this research project are presented in this section.

2.1 Materials

Agarose used for gel electrophoresis was purchased from Whitehead Scientific Pty Ltd (Cape Town, South Africa) and ethidium bromide was purchased from Promega. Acrylamide-Bis readymade solution (37.5:1) and bromophenol blue were purchased from Merck (South Africa). Ammonium persulfate, Coomassie brilliant blue G-250 powder, bovine serum albumin (BSA) and *N,N,N′,N′*-tetramethylethylenediamine (TEMED) were all purchased from Sigma (Capital Labs, South Africa). Distilled water and ultrapure water were both obtained from the Milli-Q Plus UF Ultra-Pure Water System (UKZN). Ethanol and glycerol were obtained from Saarchem (Merck, South Africa).

2.2 Quantifying DNA concentration and quality

Quantitation of nucleic acids was routinely performed to determine the concentration of DNA or RNA present in a mixture, as well as their purity. Two methods were used to establish the concentration and quality of a solution of nucleic acids namely spectrophotometric quantification and UV fluorescence in presence of a DNA dye.

2.2.1 Nanodrop

The Thermo Scientific NanoDrop 2000 UV-Vis Spectrophotometer was used for quantification of nucleic acid concentration (ng/µl) and determining its purity. A minimum of 1 µl was pipetted on the lower optical surface of the NanoDrop. Upon closing of the spectrophotometer arm, a liquid column was created between the upper and lower optical pedestal by surface tension. Nucleic acid concentration was measured following blanking the spectrophotometer with TE buffer (10 mM Tris-HCl (pH 8.0), 1 mM EDTA (pH 8.0)).

2.2.2 Agarose gel electrophoresis

Preparation of reagents

2.2.2.1 50X TAE [1X solution: 0.04 M Tris, 0.02 M acetic acid, and 0.001 M EDTA]

A stock solution of 50X TAE was made by dissolving Tris (48.4 g), glacial acetic acid (11.42 ml) and 0.5 M EDTA (20 ml) (pH 8.0) in 200 ml dH_2O.

2.2.2.2 DNA loading buffer [30% (v/v) glycerol, 0.25% (m/v) bromophenol blue]

The DNA loading buffer was made by adding bromophenol blue (0.025 g) to 3.75 ml of 80% glycerol. The volume was made up to 10 ml with dH_2O.

2.2.3 Method

To analyse the DNA samples (plasmid DNA, restriction digests and PCR products) generated in this study, agarose gel electrophoresis was used. In this procedure, agarose (1%) was completely dissolved in 1X TAE buffer in a microwave. Once the gel had cooled to approximately 45^{o}C, ethidium bromide was added to a final concentration of 0.5 μg/ml and the mixture was poured on a casting tray to set. The gel was electrophoresed (100 V, 40 min) until the bromophenol blue in the loading dye had migrated over halfway down the gel and was then viewed under UV transilluminator for analysis of DNA fragments. A standard curve of log molecular weight against the distance travelled by each fragment (cm) was plotted and band size was determined by extrapolation.

2.3 Measuring protein concentration

2.3.1 Bradford assay

The Bradford dye-binding assay is a quantitative method for the determination of protein concentration (Bradford, 1976). This method is based on the binding of Coomassie brilliant blue G-250 dye to basic amino acid side chains. The binding reaction causes a shift in the absorbance maximum of the dye from the cationic red at 465 nm to the anionic blue form at 595 nm (Compton and Jones, 1985). The intensity of the coloured reaction product is a direct function of protein concentration which can be determined by comparing its absorbance value to a standard curve.

Preparation of reagents

2.3.1.1 Standard Bovine serum albumin solution [1 mg/ml]

Bovine serum albumin (0.01 g) solution was dissolved in 10 ml of dH_2O.

2.3.1.2 Perchloric acid [2% v/v]

Perchloric acid (27.8 ml) was made up to 1 liter with dH_2O.

2.3.1.3 Bradford dye reagent

Perchloric acid (2% v/v) (1000 ml) was used to dissolve 0.6 g of Coomassie brilliant blue G-250. This was stirred for 1 hour and filtered through Whatman No. 1 filter paper and the resulting solution was stored in amber colored bottles.

2.3.2 Method

A standard protein concentration curve was constructed using bovine serum albumin ranging in concentration from 0 to 100 μg (0 – 100 μl) in Bradford reagent (to a final volume of 1 ml). The absorbance of all the solutions was measured at 595 nm after a 5 minute room temperature incubation period. This experiment was replicated in triplicate and a standard curve was generated ($R^2 = 0.9941$).

2.4 Tris-Tricine sodium dodecyl sulfate polyacrylamide gel electrophoresis (SDS-PAGE)

Tricine SDS-PAGE was intended for the resolution of smaller proteins which are sometimes poorly resolved by the commonly used Laemmli SDS-PAGE. In this system, tricine and the higher pH of the stacking gel caused the mobility of the protein relative to the trailing ion to increase, allowing for the separation of low molecular weight protein SDS complexes (Schägger and von Jagow, 1987). The protein products were made visible by the Coomassie Blue G-250 or Bradford reagent, which is the most common used anionic staining dye for proteins in SDS-PAGE gels (Dennison, 2003). Proteins in the gel were fixed by acetic acid and simultaneously stained. The excess dye incorporated into the gel could be removed by destaining with the same solution without the dye (Dennison, 2003). The proteins were detected as blue bands on a clear background.

Preparation of reagents

2.4.1.1 SDS [10% m/v]

SDS (10 g) was dissolved in dH_2O and made up to 100 ml.

2.4.1.2 Gel buffer [3 M Tris-HCl, 0.3% (m/v) SDS, pH 8.45]

Tris (72.7 g) was dissolved in dH_2O (200 ml) and adjusted to pH 8.45 with HCl. 10% (m/v) SDS (6 ml) was added and the solution was made up to 250 ml.

2.4.1.3 Anode buffer [0.2 M Tris-HCl, pH 8.9]

Tris (24.22 g) was dissolved in 950 ml of dH_2O, adjusted to pH 8.9 with HCl and made up to 1 liter.

2.4.1.4 Cathode buffer [0.1 M Tris-HCl, 0.1 M Tricine, 0.1% (m/v) SDS, pH 8.25]

Tris (12. 1 g), Tricine (17.9 g) and 10% (m/v) SDS (10 ml) were made up to 800 ml with dH_2O the pH adjusted if necessary and made to a final volume of 1 liter.

2.4.1.5 Treatment buffer [125mM Tris-HCl, 4% (m/v) SDS, 20% (v/v) glycerol, 10% (v/v) 2-mercaptoethanol, 0.01% (m/v) bromophenol blue, pH 6.8]

Stacking gel buffer (2.5 ml), glycerol (2 ml), 10% (m/v) SDS (4 ml), 2-mercaptoethanol (1 ml) and bromophenol blue 0.01% (m/v) were made up to 10 ml with dH_2O. Samples were boiled for 3 minutes in treatment buffer before electrophoresis. For non-reducing SDS-PAGE, 2-mercaptoethanol was not added.

2.4.1.6 Ammonium persulfate (APS) [10% (m/v)]

Ammonium persulfate (0.1 g) was made up to 1 ml with dH_2O. This solution was prepared before use.

2.4.1.7 Coomassie blue stain [0.125% (m/v) Coomassie brilliant blue G-250, 50% (v/v) methanol, 10% (v/v) acetic acid]

Coomassie brilliant blue G-250 powder (0.25 g), methanol (100 ml) and acetic acid (20 ml) were made up to 200 ml with dH_2O.

2.4.1.8 Destain I [50% (v/v) methanol, 10% (v/v) acetic acid]

Methanol (500 ml) and acetic acid (100 ml) were made up to 1 liter with dH_2O.

2.4.1.9 Destain II [5% (v/v) methanol, 7% (v/v) acetic acid]

Methanol (25 ml) and acetic acid (35 ml) were made up to 500 ml with dH_2O.

2.4.2 Method

The running gel consisted of dH_2O (5.05 ml), monomer solution 12.5% (v/v) (6.67 ml), gel buffer (4.0 ml), APS (0.016 ml) and TEMED (0.240 ml). This solution was poured between the glass plates and immediately overlaid with a layer of dH_2O and allowed to polymerise for 1 hour at room temperature. After polymerization, the layer of dH_2O was removed and the running gel was overlaid with stacking gel which consisted of dH_2O (3.0 ml), monomer solution 4% (v/v) (0.67 ml), gel buffer (1.25 ml), APS (0.010 ml) and TEMED (0.050 ml)]. Samples were mixed with an equal volume of treatment buffer, boiled for 3 minutes and loaded. Electrophoresis was performed at a constant current of 43 mA until the dye had migrated to the bottom of the gel. The gels were stained in Coomassie brilliant blue staining solution (section 2.4.1.7 below) overnight and subsequently destained in destain I (section 2.4.1.8) and destain II (section 2.4.1.9). After electrophoresis, the gels were soaked in Coomassie blue stain in plastic containers at room temperature and left overnight on a laboratory shaker. The following day, the Coomassie stain was then poured out and the gels were soaked in destain I until the gel background was clear. The gels were then soaked in destain II and gel images were obtained under white light using the MiniBIS PRO gel documentation system.

Chapter 3: CLONING AND PURIFICATION OF THIOREDOXIN AND THIOREDOXIN REDUCTASE

3.1 Introduction

The main challenge of isolating a protein is to choose an activity assay that can measure the presence of the protein and also distinguish it from all other proteins that may be present in the same sample (Dennison, 2003). For thioredoxin, the turbidimetric insulin reduction assay using either DTT or thioredoxin reductase/NADPH as reducing equivalent donors is used (Holmgren, 1979; Arnér and Holmgren, 2000b). In this assay, the initial velocity of the insulin reduction is derived from the linear part of the increase in absorbance at 650 nm. For thioredoxin reductase, the colorimetric reduction of 5,5′-dithiobis (2-nitrobenzoic) acid (DTNB) to 5-thio-2-nitrobenzoic acid (TNB) produces a strong yellow color at 412 nm which is measured. DTNB is very useful as a sulfhydryl assay reagent because of its specificity for thiol groups at neutral pH, high molar extinction coefficient and short reaction time (Lim and Lim, 1995).

The next challenge in protein purification is to determine a strategy for isolating the protein of choice. The method used by Seo and Lee (2010) involved three steps: ammonium sulfate fractionation, 2' 5' ADP-sepharose affinity chromatography and Sephadex G-100 column chromatography. The final choice in conventional protein purification strategy is usually a compromise between maximum recovery and maximum purity. However, one straightforward way to achieve both maxima is to fuse the target gene to a promoter which drives expression of any gene placed under its control. Furthermore, this approach allows the protein to be tagged by a His-tag, for example, to facilitate purification (Reece, 2004). The former approach was used when Kim *et al.* (2005) who cloned *TRR1* into pET-17b expression vector and subsequently induced expression of TrxR with IPTG in *E. coli* BL21 cells. TrxR was subsequently purified by diethyl aminoethyl (DEAE) and phenyl hydrophobic chromatography. Similarly, Oliveira *et al.* (2010) cloned *TRR1* into pPROEX-1 expression vector using the BamHI-NdeI restriction sites and purified by nickel affinity chromatography.

As thioredoxin is thermostable, most purification procedures make use of a heat treatment which results in the denaturation of most of the undesired proteins. This is then

subsequently followed by centrifugation and chromatography to complete the purification process. Methods implemented by Williams *et al.* (1967) in the purification of thioredoxin involved RNase A, protamine sulfate and ammonium sulfate treatments and associated centrifugation steps. Harms *et al.* (1998) were able to purify the redoxin in four basic steps which were DEAE-Sephacel anion-exchange chromatography, acid treatment with HCl**,** affinity chromatography with Procion Red and gel-permeation chromatography. Yoshiharu *et al*. (2007) were able to extract thioredoxin from *S. cerevisiae* cultured with 20% ethanol which appeared to be a promising method in thioredoxin extraction. However, because thioredoxin makes up just 0.015% of all soluble protein in yeast (Porqué *et al*., 1970) this procedure compromised maximum protein recovery (Padayachee, 2013).

In contrast, Wang *et al.* (2009) cloned *TRX1* into pLM1 expression vector using the EcoR1-Sal1 restriction sites and the resulting pLM1::TRX1 plasmid was sequenced to confirm that the construction was correct. The induced *E. coli* cells containing the pLM1::TRX1 plasmid were grown and were subsequently lysed and centrifuged. The final step of purification involved the clear supernatant being applied to a Hi-Trap column. Similarly, the *TRX1* PCR product has also been directly cloned into NotI and NdeI restriction sites of the pET28b expression vector and subsequently protein expression induced with IPTG (Zhang *et al*., 2008). Purification of the protein was done by Ni^{2+} affinity column chromatography and the purity of protein was confirmed by SDS-PAGE. Miranda-Vizuete *et al*. (1997) used a TA cloning approach and acquired the *TRX2* gene by PCR and directly ligated it into the cloning vector pGEM-T. The *Nde*I-*Bam*HI *TRX1* fragment from this vector was subsequently sub-cloned into the pET-15b expression vector system. The protein was purified by applying the clear supernatant from the lysed centrifuged cells through a Hi-Trap column. The materials and methods used to isolate and purify components of the thioredoxin systems for subsequent kinetic analysis are described below.

3.2 Materials and methods

3.2.1 Materials

RNase A was obtained from Roche (South Africa). The Thermo Scientific Rapid DNA Ligation Kit, Fermentas Gel Extraction Kit, InsTAclone™ PCR cloning kit, TransformAid™ Bacterial Transformation Kit, 100 bp plus and 1 kbp Molecular Weight Markers and Taq™ DNA polymerase were obtained from Inqaba Biotech (Johannesburg,

South Africa). Kanamycin, ampicillin and Isopropyl β-D-1-thiogalactopyranoside (IPTG) were from Sigma (Capital Labs, South Africa) while the QIAquick™ Gel Extraction Kit and Ni-NTA agarose were from Whitehead Scientific (Pty) Ltd (Cape Town, South Africa). The New England Biolabs restriction enzymes HindIII, NdeI and BamHI were obtained from The Scientific Group (Midrand, South Africa). *Escherichia coli* BL21 (DE3) and DH5α cells were acquired from Megan Brunkhorst (Genetics, UKZN). The expression vector, pET28a, was from the Biochemistry department (UKZN) and the thioredoxin clones (LPTRXA and B) were generously supplied by Miss L. Padayachee (PhD candidate, UKZN). All other common reagents were obtained from Saarchem (Merck, South Africa).

3.2.2 Preparation of reagents

3.2.2.1 Kanamycin [30 mg/ml]

Kanamycin sulphate (0.3 g) was dissolved in dH_2O and the volume was made up to 10 ml. The suspension was sterilized filtering through a 0.2 μm filter and stored in 1 ml aliquots at -20^oC.

3.2.2.2 Ampicillin [25 mg/ml]

Ampicillin sodium salt (0.25 g) was dissolved in dH_2O and the volume was made up to 10 ml. The suspension was sterilized by passing it through a 0.2 μm filter and stored in 1 ml aliquots at -20°C.

3.2.2.3 Isopropyl β-D-1-thiogalactopyranoside (IPTG)

IPTG powder (0.238 g) was dissolved in dH_2O and the volume was made up to 10 ml. This suspension was sterilized by passing it through a 0.2 μm filter and stored in 1 ml aliquots at -20^oC.

3.2.2.4 Luria Bertani (LB) agar

Yeast extract 0.5% (w/v), tryptone 1% (w/v), NaCl 0.5% (w/v) and bacteriological agar 1.5% (w/v) were dissolved in dH_2O and the solution was made up to the desired volume. The solution was autoclaved and allowed to cool. Kanamycin (30 μg/ml) or ampicillin (100 μg/ml) was added to the required final concentration and plates were then poured and stored in the fridge at 4°C.

3.2.2.5 Luria Bertani (LB) broth

Tryptone 1% (w/v), NaCl 0.5% (w/v) and yeast extract 0.5% (w/v) were dissolved in dH_2O and the solution was made up to the desired volume. The solution was autoclaved and allowed to cool. Kanamycin (30 µg/ml) or ampicillin (100 µg/ml) was added to the required final concentration.

3.2.2.6 SOC media

Tryptone 2% (w/v), yeast extract 0.5% (w/v), $MgCl_2$ (10 mM), NaCl (10 mM) and KCl (2.5 mM) were dissolved in dH_2O and the solution was made up to the desired volume. The solution was autoclaved and cooled. Glucose was added to the desired final concentration [20 mM]. Prior to addition, the glucose stock solution (1 M) was sterilized by filtration through a 0.2 µm filter. The SOC media was stored at 4°C.

3.2.2.7 2xYT media

Tryptone 1.6% (w/v), yeast extract 1% (w/v) and NaCl 0.5% (w/v) were dissolved in dH_2O. The pH was adjusted to 7.0 with NaOH and the volume was made up with dH_2O. The solution was sterilized by autoclaving and thereafter stored at room temperature.

3.2.2.8 Yeast Peptone Dextrose (YPD)

Peptone 2% (w/v), dextrose 2% (w/v) and yeast extract 1% (w/v) were dissolved in dH_2O and the solution was made up to the desired volume and the solution was autoclaved.

3.3 Methods

3.3.1 Cloning of TrxR

The following methods where used for cloning of TrxR.

3.3.1.1 Isolation of yeast genomic DNA

Genomic DNA from *Saccharomyces cerevisiae* was extracted from 4 x 1.5 ml overnight cultures grown in YPD using the Bust ‘n Grab method (Harju *et al*., 2004). The overnight cultures were pelleted (20, 000 x *g* for 5 minutes, room temperature) and the pellet was re-suspended in lysis buffer (2% (v/v) Triton X-100, 1% (w/v) SDS, 100 mM NaCl, 10 mM Tris-HCl (pH 8.0) and 1 mM EDTA (pH 8.0)) by gentle inversion of the tubes or

brief vortex if needed. Sequential rapid freeze-thaw steps (-75^{o}C for 5 minutes and 95^{o}C water bath for a minute) were followed by 30 seconds of vortexing. Chloroform (200 µl) was added to the tubes followed by 2 minutes of vortexing. The tubes were centrifuged (20, 000 x *g,* 5 minutes, room temperature) and three distinct layers could be seen. The upper aqueous phase was transferred into a clean eppendorf tube containing 400 µl ice-cold 100% (v/v) ethanol. The tubes were inverted and incubated for 5 min at -20°C in order to precipitate the DNA. The precipitated DNA was pelleted by centrifugation (20, 000 × *g*, 5 minutes, room temperature), washed with 70% (v/v) ethanol (0.5 ml) and air-dried. The pellets were re-suspended in 50 µl TE buffer [1 mM EDTA (pH 8.0), 10 mM Tris-HCl (pH 8.0)] and the samples were assayed by the Nano Drop 2000 UV-Vis Spectrophotometer and agarose gel electrophoresis to determine DNA concentration and purity.

3.3.1.2 PCR

3.3.1.2.1 Plasmid and genomic DNA

To amplify the *TRR1* gene from genomic DNA and to confirm the identity of the plasmid DNA, PCR was performed using yeast *TRR1* specific primers, 5'-AGC**CATATG**GTTCACAACAAAGTTAC-3' and 5'-ACG**AAGCTTATT**CTAGGGAAGTTAAGT-3' (NdeI and HindIII sites are underlined) which were designed using Primer3 (http://frodo.wi.mit.edu). The PCR reaction mixture consisted of TaqDNA polymerase (0.5 U), reaction buffer (1X), a dNTP mix (0.2 mM), the forward and reverse primers (250 nM each) and plasmid or genomic DNA (0.01-1 µg) in 25 µl. The following PCR cycling conditions were used: 94°C, 1 min (initial denaturation); 94°C, 30sec; 46°C, 30 sec; 72°C, 1 min (35 cycles) and a final extension of 72°C, 5 min. A no template control was included in order to check for contamination and the PCR products were analyzed by agarose gel electrophoresis (100 V, 65 A; Section 2.2.2).

3.3.1.2.2 Colony PCR

Small sections of the single colonies from different test plates were selected, dissolved in autoclaved dH_2O (25 µl) and incubated in a water bath (2 min, 100^{o}C). The tubes were centrifuged (13, 000 × *g*, 2 min, room temperature) and 2 µl of the supernatant was used to perform a PCR as described above (section 3.3.1.2.2).

3.3.2 Plasmid DNA purification

Plasmid DNA was purified using a standard mini-prep procedure (Sambrook *et al*., 1989). Four 10 ml samples of an overnight culture grown in LB containing the appropriate antibiotic were centrifuged (7250 × *g,* 5 min, 4°C) and the pellet was re-suspended in 200 µl GTE solution (25 mM Tris-Cl (pH 8.0), 10 mM EDTA, 50 mM glucose). RNase A (2 µg/ml) was then added and the suspension was incubated at room temperature for 5 min and subsequently transferred into a sterile eppendorf tube. 400 µl of a NaOH/SDS solution (0.2 M NaOH, 1% (w/v) SDS) was added to lyse the cells and the suspension was mixed by gentle finger tapping followed by incubation on ice for 5 min. A 3 M potassium acetate solution (300 µl) was added and the suspension was incubated on ice for 5 min before being centrifuged (12 000 x *g*, 5 min, room temperature). Isopropanol (600 µl) was added to the supernatant (800 µl) which was incubated at -20°C for 30 min. The suspension was centrifuged (12 000 × *g*, 5 min, room temperature) and the pellet was washed with ice-cold 70% ethanol (500 µl). The pellet was then re-suspended in 50 µl TE buffer (10 mM Tris-HCl (pH 8.0), 1 mM EDTA (pH 8.0)). These samples were assayed using a Nano Drop 2000 UV-Vis Spectrophotometer and by agarose gel electrophoresis to determine DNA concentration and purity.

3.3.3 Restriction digestion

Plasmid DNA was routinely restricted with BamHI or HindIII to linearize the DNA for sizing. In these reactions, plasmid DNA (1 µg), restriction enzyme (1 U) and buffer were incubated at 37^{o}C for 1 hour. For cloning experiments, plasmid DNA was restricted with HindIII and NdeI to liberate the *TRR1* fragment. In these reactions, plasmid DNA (240 ng/µl), restriction enzyme (1 U each) nuclease free water and BSA (4 µg/µl) were all incubated with 1X NEBuffer 2 at 37^{o}C for 3 hours.

3.3.4 Gel purification of the TRR1 insert and pET28a vector

Restriction digested pET28a and the liberated *TRR1* fragment were both gel purified using a QIAquick Gel Extraction Kit or the Fermentas Gel Extraction Kit as per manufacturer's instructions.

3.3.5 Ligation of TRR1 insert into plasmid vectors

A typical ligation mixture contained vector DNA (10 – 100 ng), insert DNA (at 3: 1 molar excess over vector), 1X Rapid Ligation Buffer, T4 DNA ligase (5U/µl) and nuclease free water. The mixture was then incubated at room temperature for an hour followed by an overnight incubation at 4^{o}C and was then used for transformation.

3.3.5.1 InsTAcloning T-vector

The pTZ57R/T vector was transformed into *E. coli* JM109 cells using the TransformAid^{TM} Bacterial Transformation Kit according to the manufacturer's instructions and yielded clones (pTRRA, B, C, and D). As a positive control for competent cell growth, *E. coli* JM109 competent cells were plated onto LB agar plate with no antibiotic and as a negative control, untransformed cells were plated onto LB plates containing ampicillin (100 µg/ml). In order to purify the recombinant pTZ57R/T DNA, a plasmid mini-prep procedure was (section 3.3.2).

3.3.5.2 pET28a

The gel-extracted *TRR1* fragment and restricted pET28a expression vector were ligated (section 3.3.5) to form the expression plasmids pMTRA, B, C and D using a Rapid DNA Ligation Kit and this was plated onto LB agar plates containing kanamycin (30 µg/ml). As a positive control for competent cell growth, *E. coli* BL21 (DE3) competent cells (section 3.3.6.1) were plated onto LB agar plates with no antibiotic and as a negative control, untransformed cells were plated onto LB plates containing kanamycin (30 µg/ml). In order to purify the recombinant DNA (pMTRA – D), a plasmid mini-prep procedure was performed as per section 3.3.2.

3.3.6 Transformation

3.3.6.1 Generation of competent cells ($CaCl_2$)

A calcium chloride ($CaCl_2$) method was used to make *E. coli* BL21 (DE3) competent cells (Sabel'nikov *et al*., 1977). *E. coli* BL21 (DE3) cells were grown in 2xYT medium (Tryptone 1.6% (w/v), yeast extract 1% (w/v) and NaCl 0.5% (w/v)) until an OD_{600} 0.3-0.4 was reached. Four 10 ml samples were transferred to ice-cold sterile tubes, incubated on ice for 10 min and thereafter centrifuged (4500 × *g*, 10 min, 4°C). The pellet was re-suspended in

ice-cold 0.1 M calcium chloride (10 ml). The suspension was centrifuged (4500 x *g*, 10 min, 4°C) and the pellet was re-suspended in ice-cold 0.1 M calcium chloride (2 ml) followed by a 30 min incubation on ice. These competent cells were made just before transformation for better efficiency.

3.3.6.2 Transformation of the pET28a-TrxR clones

The ligation mix (5 µl) was added to competent cells (20 µl) and incubated on ice (30 min). This mixture was then heat shocked (42^{o}C, 90 s) and placed directly on ice (2 min). Pre-warmed (37^{o}C) SOC media (Tryptone 2% (w/v), yeast extract 0.5% (w/v), $MgCl_2$ (10 mM), NaCl (10 mM), KCl (2.5 mM) and glucose (20 mM)) (80 µl) was added to the cells which were incubated for 1 hour at 37^{o}C in a shaking water bath. The transformation mix (50 µl) was plated onto LB agar plates containing 100 µg/ml of ampicillin and incubated at 37^{o}C overnight. As a control for competent cell growth, *E. coli* BL21 (DE3) competent cells were plated onto a LB agar plate (no antibiotic) whilst as a control for antibiotic activity, untransformed *E. coli* BL21 (DE3) competent cells plated onto the selective medium. As a control for competency, *E. coli* BL21 (DE3) cells were transformed with the pET28a expression vector (50 ng) and the transformation efficiency was calculated. To confirm the identity of the clones obtained, a colony PCR using the reaction conditions described above was done and the plasmid DNA was purified and linearized with NdeI or BamHI (Section 3.3.3).

3.3.7 Induction, expression and purification of thioredoxin and TrxR

3.3.7.1 Generating a crude extract for purification

3.3.7.1.1 Induction and expression

Protein expression of the pET28a clones (pMTRA, B, C and D), was induced by culturing selected clones in LB kanamycin (30 µg/ml) media until an OD_{600} of between 0.3-0.4 was reached. IPTG (0.5 mM) was added to cultures which were incubated at 37^{o}C in a shaking water bath. Following IPTG addition, samples were taken every 30 minutes and an OD_{600} measured. These samples were centrifuged (12,000 × *g*, 10 min, 4^{o}C) and re-suspended in water to a final OD_{600} of 10. An equal amount of treatment buffer [125mM Tris-HCl, 4% (m/v) SDS, 20% (v/v) glycerol, 10% (v/v) 2- mercaptoethanol, 0.01% (m/v)

bromophenol blue, pH 6.8] was added to 20 µl of the re-suspended samples and the samples were analyzed by SDS-PAGE.

3.3.7.1.2. Sonication

Sonication is the use of high intensity sound waves to disrupt cells and thus allowing protein extraction from cells (Benov and Al-Ibraheem, 2002). Samples (OD_{600} of 10) were sonicated for 2 minutes and incubated on ice for 1 minute. This was repeated three times and thereafter, the samples were centrifuged (15, 000 × g, 30 min, 4^{o}C) and the supernatant was stored at -20^{o}C.

3.3.7.2 Ni-NTA affinity purification

Ni-NTA agarose beads (1 ml) were added and allowed to settle into a column and equilibrated with 5 volumes equilibration buffer (0.02 M imidazole, 0.5 M NaCl, 0.001 M mercaptoethanol, 0.02 M Tris-HCL (pH 8.0)). The column was incubated with the appropriate crude extract (thioredoxin or thioredoxin reductase) at 4°C overnight in a Revolver™ 360° Sample Mixer. The unbound fraction was thereafter eluted and the resin was washed with 10 volumes of wash buffer (0.5 M NaCl, 0.02 M Tris-HCl (pH 8.0)). Two volumes of elution buffer (0.25 M imidazole, 0.5 M NaCl, 0.02 M Tris-HCl (pH 8.0)) were then incubated with the resin (4°C, 30 min) and the bound protein was eluted and the resulting fractions were analyzed by SDS-PAGE (Section 2.4). The resin was then washed with 0.5 M NaOH for 30 min and stored in 30% (v/v) ethanol at 4°C.

3.4 Results

3.4.1 Cloning of thioredoxin reductase from *Saccharomyces cerevisiae*

To clone the *TRR1* gene, genomic DNA was isolated from *S. cerevisiae* using the Bust ‘n Grab method (Figure 3.1 A; Harju *et al*., 2004) and PCR amplification of the *TRR1* gene was performed using *TRR1* specific primers (Figure 3.1 B). The resulting PCR amplicons were gel purified (Figure 3.4.1 C) and sized at the expected size of 960 bp.

The gel purified *TRR1* fragment was then ligated to the pTZ57R/T vector using the InsTAcloneTM PCR cloning kit and transformed into *E. coli* JM109 cells yielding four clones (pTRRA-D). Plasmid DNA from these clones was isolated using a plasmid DNA isolation procedure (Figure 3.1 D).

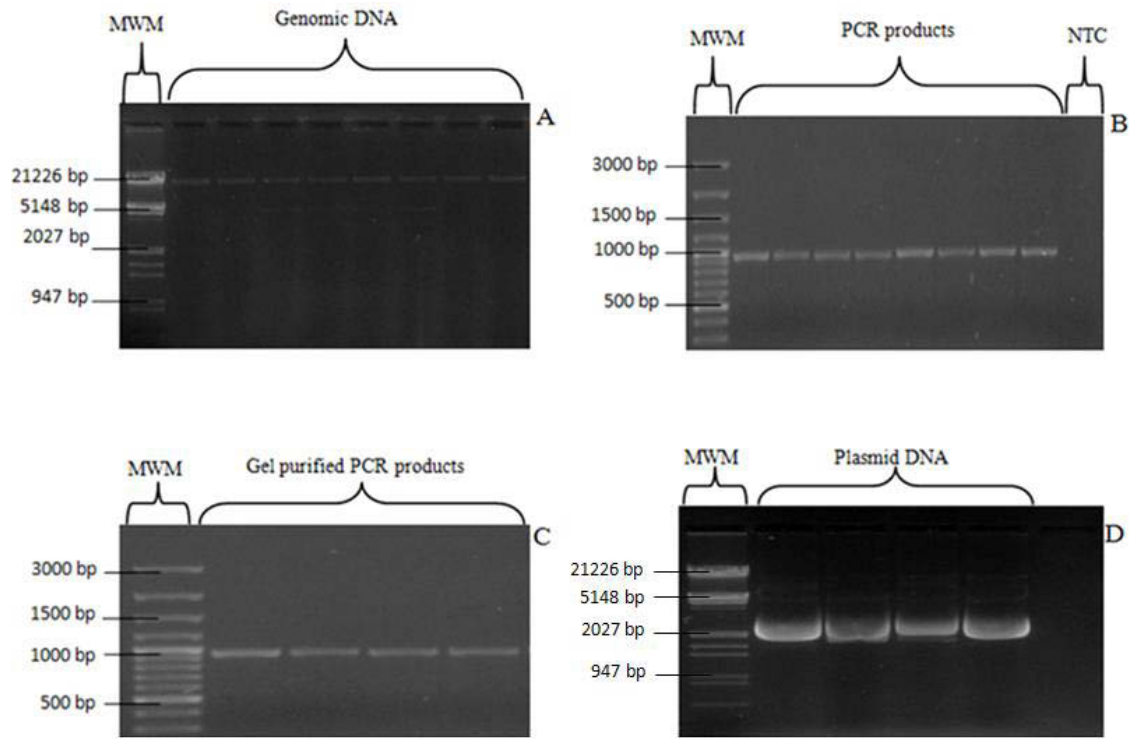

Figure 3.1 TA cloning of TRR1 from *S. cerevisiae*. Genomic DNA was isolated from S. cerevisiae using the Bust 'n Grab procedure (Harju *et al*., 2004) (A), PCR of the DNA was undertaken using TRR1-specific primers and a no template control (NTC) was included to check for the presence of contamination (B), PCR product was gel purified using the Fermentas gel purification kit (C) and the plasmid DNA of the clones was isolated using the plasmid DNA purification (Section 3.3.2) (D).

The isolated plasmid DNA from these clones was used to confirm the identities of the clones by using two approaches. Firstly, restriction digestion using NdeI and HindIII was performed using the plasmid DNA of the pTRRA-D clones to liberate the *TRR1* fragment. This restriction digestion showed that the size of the bands obtained were 2890 bp (pTZ57R/T), 966 bp (*TRR1* fragment) and 3823 bp (pTRRA clone without the HindIII to HindIII site on the pTZ57R/T vector) matched the expected band sizes 2886 bp (pTZ57R/T), 960 bp (*TRR1* fragment) and 3846 bp (pTRRA clone without the HindIII to HindIII site on the pTZ57R/T vector) (Fig. 3.2 A). Secondly, a PCR with *TRR1*-specific primers was performed using the pTRRA-D plasmid DNA as a template. The amplicons (966 bp) obtained showed that *TRR1* was present in the pTRRA-D vectors (Fig. 3.2 B).

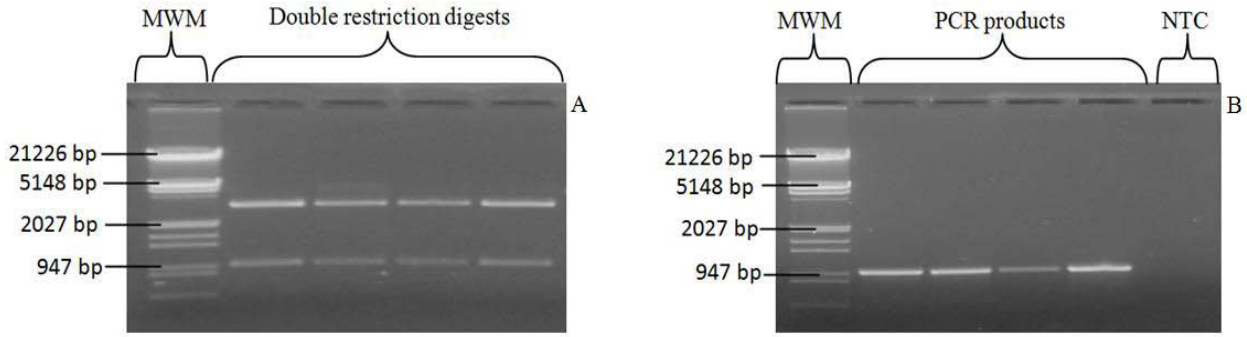

Figure 3.2 Confirming that the pTRRA-D clones contained *TRR1*. The isolated pTRRA-D clones were restricted with NdeI and HindIII (A). In addition, PCR of the plasmid DNA was undertaken using *TRR1*-specific primers to confirm the presence of the insert and a no template control (NTC) was included (B).

The expression vector, pET28a, was isolated from *E. coli* BL21 (DE3) cells using the standard plasmid DNA purification procedure (Section 3.3.2) and a double digestion with NdeI and HindIII was performed so that the similarly cut *TRR1* fragment could be ligated into the expression vector (Fig. 3.3).

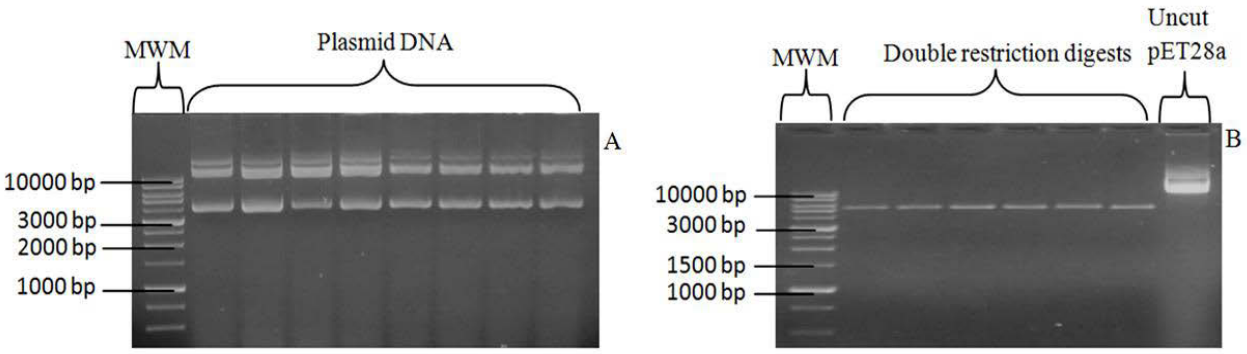

Figure 3.3 Isolation and restriction digest of expression vector for sub-cloning. pET28a was isolated from *E. coli* BL21 (DE3) (A) and restriction digested with the NdeI and HindIII restriction enzymes and an uncut pET28a control was included (B).

The gel purified *TRR1* fragments and the restricted pET28a vector DNA were ligated using a 3:1 molar ratio of insert to vector DNA to yield the plasmids pMTRA-D. A one-hour ligation incubation at room temperature followed by overnight incubation at 4^{o}C was sufficient for these experiments. The pMTRA-D vector DNA was then transformed into competent *E. coli* BL21 (DE3*)* cells (Section 3.3.6.1) and plated on LB kanamycin plates.

To select for clones containing pMTRA-D, single colony PCR (Section 3.3.1.2.2) was performed using a small fraction of the selected colonies. The results showed that the *TRR1* fragment had been successfully ligated to pET28a (Fig. 3.4 A) and a PCR was performed using the plasmid DNA (B) as a template. The amplicons (967 bp) obtained showed that *TRR1* had indeed been successfully ligated into pET28a (Fig. 3.4 C). A restriction digestion to liberate the *TRR1* fragment out of the pET28a vector (Fig. 3.4 D) was also performed and the sizes of the bands obtained 970 bp (*TRR1* fragment) and 5370 bp (pET28a) matched the expected sizes 960 bp (*TRR1* fragment).

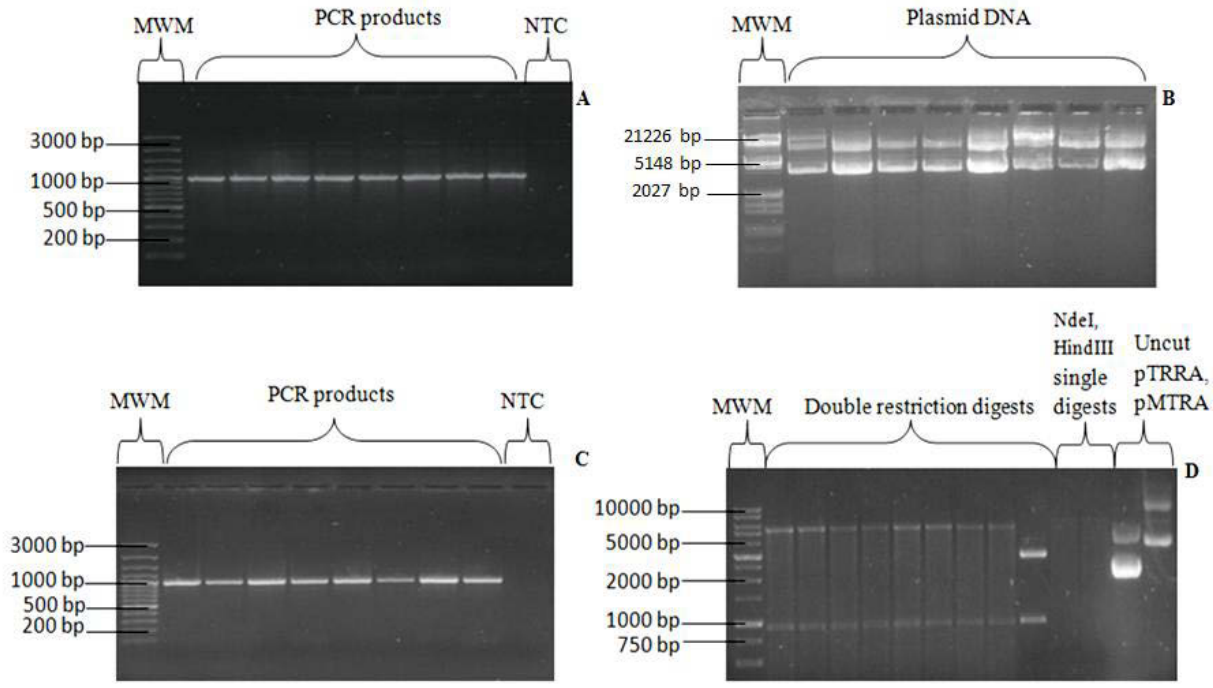

Figure 3.4 Confirming that the pMTRA-D clones contained *TRR1*. A colony PCR was performed using a small fraction of the single colonies and a NTC was included (A). pMTRA-D DNA was isolated from *E. coli* BL21 (DE3) cells using a plasmid DNA procedure (B). A PCR of the plasmid DNA was undertaken using *TRR1*-specific primers to confirm the presence of the insert in the plasmid isolations and a NTC was also included (C). Plasmid DNA of the clones was restriction digested with HindIII and NdeI. Control experiments included a restriction digestion with NdeI and HindIII on pTRRA, single restriction digestions with NdeI and HindIII and the uncut pTRRA and pMTRA (D).

Figure 3.5 Sequence alignments of the pMTRA promoter sequences with the *TRR1* sequence from *S. cerevisiae* by ClustalW2. The pMTRA-Dclones were sequenced (Central Analytical Facilities, Stellenbosch University) in both directions (promoter and terminal) and the sequence data was evaluated (Fig. 3.5). All of the four sequences were aligned to the *TRR1* sequence from the Saccharomyces Genome Database (SGD) (http://www.yeastgenome.org, Gene ID: 851955).

3.4.2 Induction, expression and purification of thioredoxin reductase from the pMTRA-D clones

After confirmation of the identity of the pMTRA–D clones, protein expression was induced in these cells with IPTG. In these experiments, IPTG was added to the cultures (Section 3.3.7.1.1) and protein expression was monitored periodically (30-180 min). A comparison of the uninduced control and the induced sample showed the enhanced expression at 36 kDa which was close to the expected size of 35 kDa for TRR1 (Fig. 3.6). The maximum expression of thioredoxin reductase was observed at the 60 min interval and this time point was used in the purification of the protein.

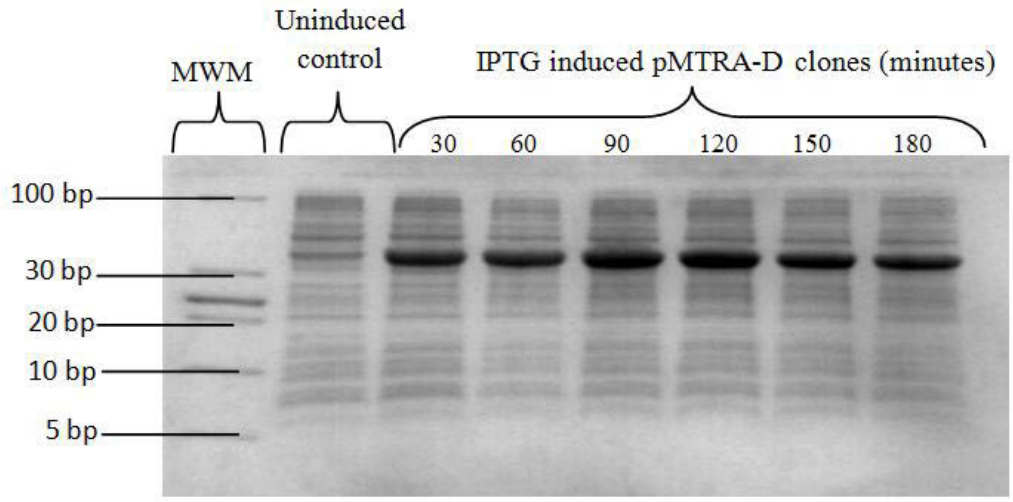

Figure 3.6 IPTG induced expression of the pMTRA-D clones. The clones were induced with 0.5 mM isopropyl β-D-1-thiogalactopyranoside (IPTG) for various time intervals (0-180 min). To ensure that an equal amount of protein was loaded into each well, samples from the induced cultures were diluted to an equal optical density of 10 before sample buffer was added to them. An uninduced control was included.

To purify the recombinant thioredoxin reductase, transformed *E. coli* BL21 (DE3) cells were cultured and induced with IPTG (0.5 mM) for 60 min. The samples were then centrifuged (12,000 × *g*, 10 min, 4^{o}C) and re-suspended in water to a final OD_{600} of 10. An equal amount of treatment buffer [125mM Tris-HCl, 4% (m/v) SDS, 20% (v/v) glycerol, 10% (v/v) 2- mercaptoethanol, 0.01% (m/v) bromophenol blue, pH 6.8] was added to 20 µl of the re-suspended samples (Section 3.3.7.1) and the crude extract was used for nickel affinity chromatography (Section 3.3.7.2). The absence of bands from the wash procedure and

appearance of single bands (Fig. 3.7) show successful purification of thioredoxin reductase with a size of 35 kDa (Fig. 3.6).

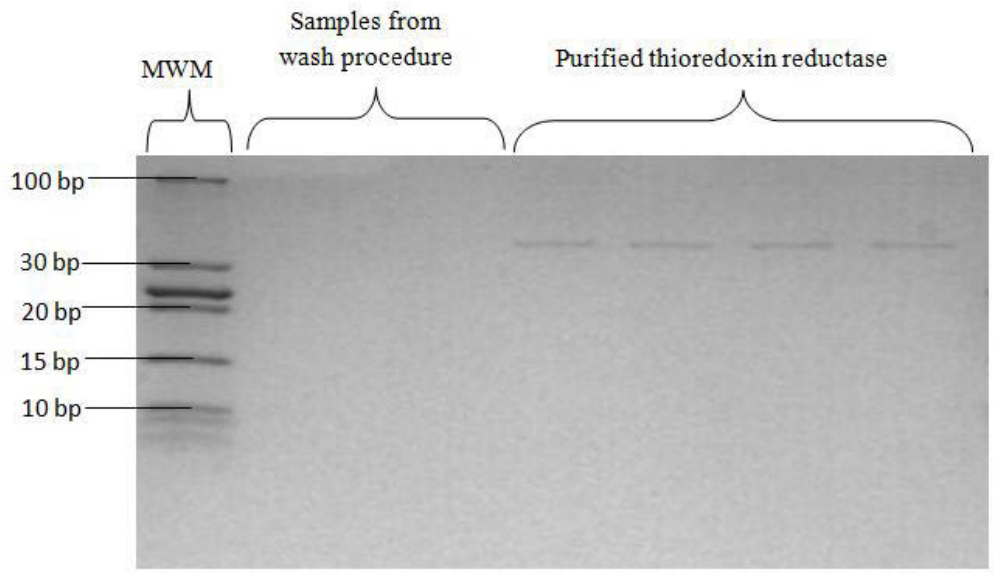

Figure 3.7 Purification of recombinant thioredoxin reductase by nickel affinity chromatography. *TRR1* was induced for 1 hour and the induced cells were treated as described in section 3.3.7.1 for protein purification. Samples from the wash procedure of Ni-NTA affinity purification were included.

3.4.3 Induction, expression and purification of thioredoxin from the *pLPTrxA/B* clones

The pLPTrxA-B clones were obtained from Miss L. Padayachee (PhD student, UKZN). To confirm the identity of these clones, sequence analysis (Central Analytical Facilities, Stellenbosch University) was also performed on them (data not shown). Following sequence analysis, the clones (pLPTrxA-B) were IPTG-induced at different time intervals (data not shown) and the optimal expression period was shown to be 6 hours. The protein was expressed successfully with the induced bands at a calculated size of 13 kDa which was very close to the expected size of 12 kDa (Fig. 3.8)

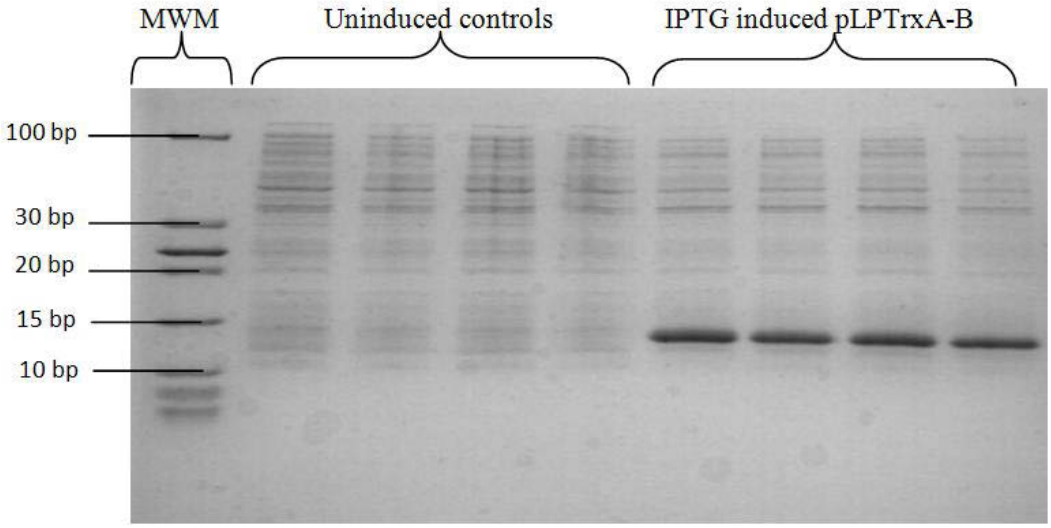

Figure 3.8 IPTG induced expression of the pLPTrxA-B clones. Clones were induced with 0.5 mM isopropyl β-D-1-thiogalactopyranoside (IPTG) for 6 hours. To ensure that an equal amount of protein was loaded into each well, samples from the induced cultures were diluted to an equal optical density of 10 before sample buffer was added to them. The uninduced samples were included.

Similarly as described for to the recombinant purification of thioredoxin reductase, transformed *E. coli* (DE3) cells containing the pLPTrxA-B clones was cultured and induced with IPTG for 6 hours as this is when optimum protein expression is observed (Padayachee, 2013). These samples were then treated as described above (Section 3.3.7.1) and used as crude extract for nickel affinity chromatography (Section 3.3.7.2). The absence of bands from the wash procedure and appearance of single bands (Fig. 3.9) show successful purification of thioredoxin with size 12 kDa (Fig. 3.9).

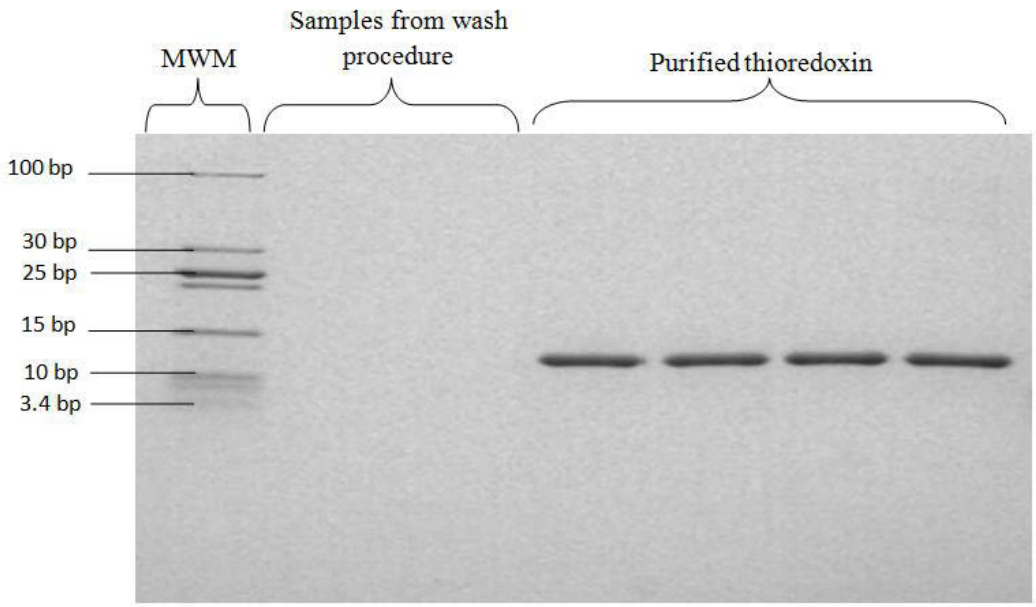

Figure 3.9 Purification of recombinant thioredoxin by affinity chromatography. After *TRX1* had been induced for 6 hours, the cells were treated as described in section 3.3.7.1 for protein purification. Samples from the wash procedure of Ni-NTA affinity purification were included.

3.5 Discussion

One of the major hurdles that had to be overcome in this research was acquiring pure thioredoxin and thioredoxin reductase which are extremely costly and we therefore chose to purify these proteins. In native protein purification, thioredoxin was harvested from supernatants of yeast cells incubated with 20% (v/v) ethanol at 37°C for 2 hours and were secreted directly into the medium after the incubation period (Inoue *et al.,* 2007). This method could offer several advantages as opposed to conventional extraction methods. However, Inoue *et al*., (2007) utilized Western blotting instead of SDS-PAGE for their analysis of purified protein and studies in our lab found that the yield obtained from this method was very low and therefore recombinant expression was investigated (Padayachee, 2013). On the other hand, recombinant expression, *E. coli* offers a means for the rapid, high yield production of thioredoxin system proteins.

In this study, genomic DNA from *S. cerevisiae* was successfully isolated (Fig. 3.1 A) and the *TRR1* gene was amplified (Fig. 3.1 B) and cloned into the pTZ57R/T cloning vector. *TRR1* was then subcloned into the pET28a expression vector. The successful induction of thioredoxin reductase expression (Fig. 3.6) and the sequence data alignments (Fig. 3.5) proved that *TRR1* was successfully cloned and expressed. Thioredoxin clones were acquired (as

mentioned in section 3.2) and tested and these were found to contain the *TRX1* gene and thus expression was induced in these cells (Fig. 3.8). Both thioredoxin (Fig. 3.9) and thioredoxin reductase (Fig. 3.7) were subsequently purified using nickel affinity chromatography. The purified proteins were then ready to be assayed and used in our kinetic analysis.

Future studies could use of high-cell-density protein expression methods including auto-induction introduced by Studier (2005) or a high-cell-density IPTG-induction method (Sivashanmugam *et al*., 2009). With the latter method, 14–25 mg of NMR triple-labeled proteins and 17–34 mg of unlabeled proteins from a 50 mL cell culture was easily obtainable and this high protein yield used the same recombinant DNA constructs, bacterial strains and a regular incubator shaker (Sivashanmugam *et al*., 2009). In the former method, high-density protein expression was achieved by simply inoculating a suitable auto-inducing medium from a seed culture and growing to saturation. This produced much higher levels of target protein per volume of culture compared to IPTG or other inducer dependent expression (Studier, 2005).

Chapter 4: THIOREDOXIN DEPENDENT REACTIONS ARE INTERCONNECTED?

4.1 Introduction

The main aim of this study was to determine the interconnectivity of thioredoxin dependent reactions. In previous computational modeling studies, it was shown that changes in the activity of some reactions affected the fluxes of other reactions in the thioredoxin system (Pillay *et al*., 2011). However, as stated in chapter 1, these results were obtained solely from computational analysis and it is not known whether the system displays this behaviour *in vitro* and *in vivo.* Thus, to confirm these computational results, the system was analysed *in vitro*. As a first step to describe the connectivity between thioredoxin-dependent reactions precisely, a reaction scheme describing the oxidation of thioredoxin by two substrates and its subsequent reduction by thioredoxin reductase was developed and analyzed in this study (Fig. 4.1).

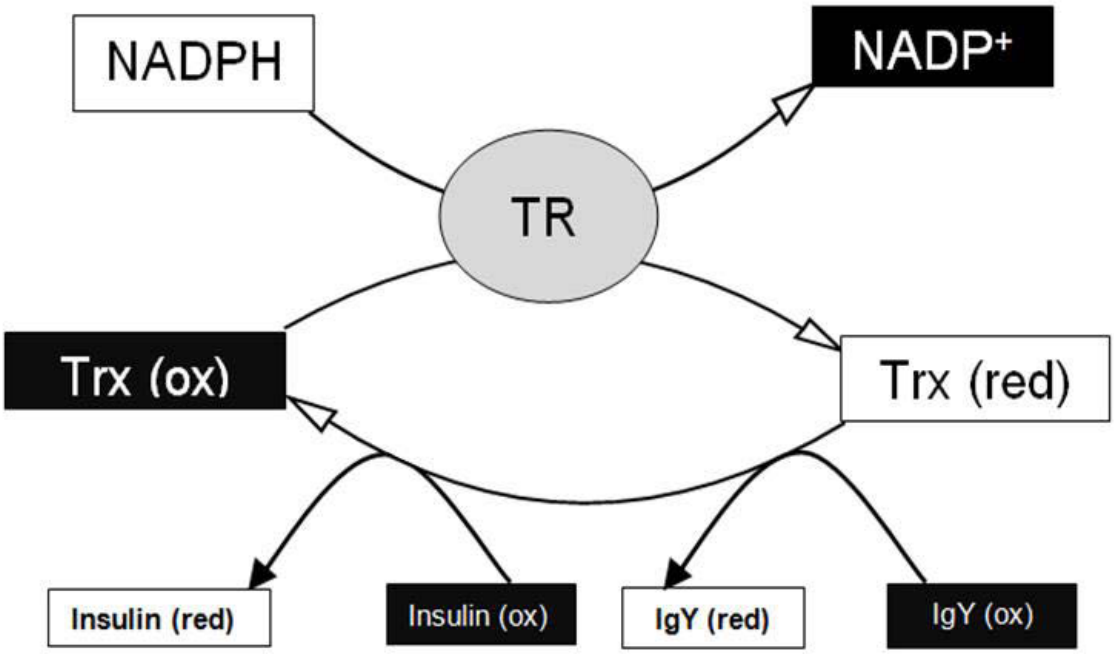

Figure 4.1 Reaction scheme of the proposed thioredoxin competition assay. The reduced thioredoxin, Trx (red), directly interacts with oxidized proteins Insulin (ox) and IgY (ox) by reducing disulfide bridges. As a result, the target protein is reduced (Insulin (red)) and IgY (red) and thioredoxin itself is oxidized (Trx (ox)). The regeneration of thioredoxin from its oxidized form is catalyzed by thioredoxin reductase (TR) using NADPH.

For this assay, two substrates of thioredoxin had to be obtained. In previous kinetic assays, it was shown that the DTT-dependent reduction of insulin increased in the presence of thioredoxin, suggesting that Trx catalysed the rate of insulin reduction (Holmgren, 1979). This reduction of insulin by the thioredoxin system can be measured in two ways. Firstly, the rate of NADPH oxidation can be monitored by the decrease in absorbance at 340 nm (Holmgren, 1979). As the reduction reaction proceeds, a white precipitate is formed mainly from the free insoluble β-chains of insulin which allows for a second method to determine thioredoxin system activity (Holmgren, 1979). The formation of that precipitate causes turbidity in the mixture which can be recorded spectrophotometrically at 650 nm (Holmgren, 1979).

The competing substrate used in this study, immunoglobin Y, was chosen as it contains disulfide bonds (Fig. 4.2) and is readily obtained (Pürzel *et al.*, 2009). Although this substrate had never been tested before, it was expected that thioredoxin would also have a similar reducing activity on IgY.

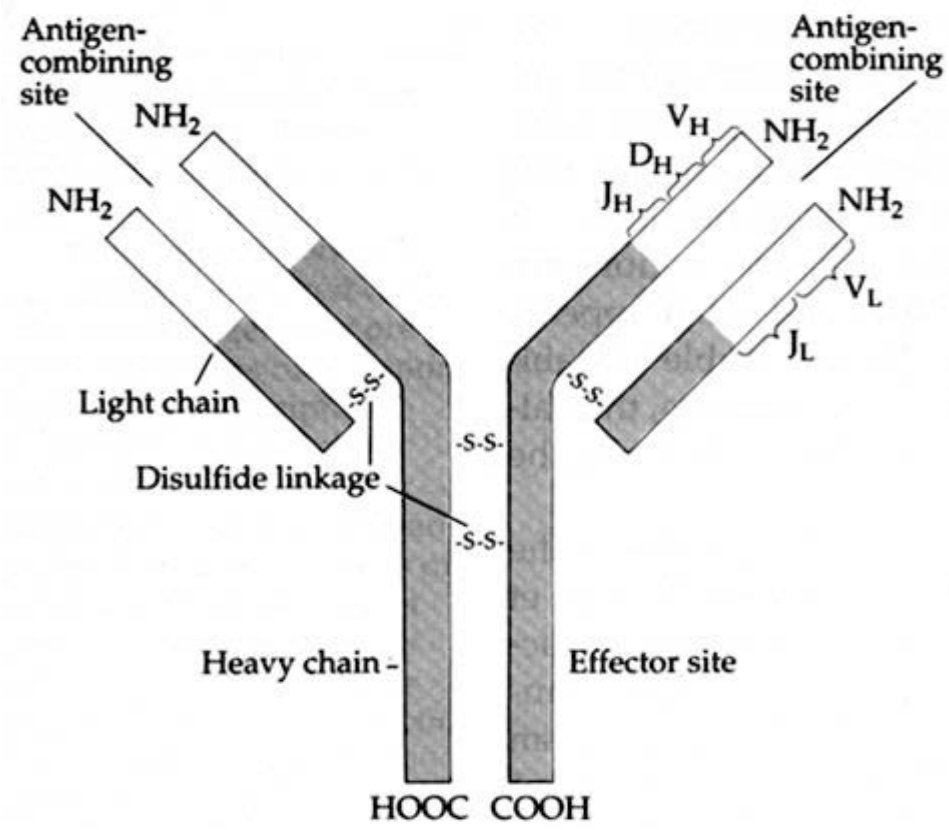

Figure 4.2 Structure of a typical immunoglobulin (antibody) protein. Two identical heavy chains are connected by disulfide linkages (Gilbert, 2010).

Like other immunoglobins, IgY is a Y-shaped molecule (Fig. 4.2) that consists of two identical heavy chains and two identical light chains which are connected by disulfide bonds (Woof and Burton, 2004). It is a major antibody found in birds, reptiles and lungfish blood (Leslie and Clem, 1969). However, for the purpose of this study, IgY was isolated from chicken egg yolks as they were easily obtainable.

The effect of IgY reduction by thioredoxin was also to be determined in a similar fashion to that of insulin by monitoring NADPH oxidation at 340 nm. However, if IgY oxidation did not result in turbidity, then it would be possible to monitor the overall flux in the system through NADPH oxidation at 340 nm and the reduction of insulin specifically at 650 nm. Thus, if IgY acted as a competitive inhibitor for insulin reduction, then the rate of turbidity at 650 nm should decrease with increasing IgY concentrations.

4.2 Materials and methods

4.2.1 Materials

Dithiothreitol (DTT), human recombinant insulin, 5, 5'-dithiobis (2-nitrobenzoic acid) (DTNB), β-nicotinamide adenine dinucleotide phosphate (NADPH), bovine serum albumin (BSA) were obtained from Sigma (Capital Labs, South Africa). Polyethylene glycol (PEG) 20,000 was obtained from Merck (South Africa) and all other common reagents were obtained from Saarchem (Merck, South Africa).

4.2.2 Preparation of reagents

4.2.2.1 Human recombinant insulin [1.6 mM]

A stock solution of insulin was prepared by dissolving insulin (50 mg) in 0.5 ml of 100 mM potassium phosphate buffer (pH 6.5). The pH was adjusted to 2-3 with 1 M HCl and thereafter titrated back to the original pH of the buffer (pH 6.5) with NaOH (1 M). The volume was then adjusted to 5 ml with dH_2O and the solution was stored at – 20°C.

4.2.2.2 DTNB [63.1 mM]

A stock solution of DTNB was prepared (before use) by dissolving DTNB powder (0.025 g) in 99% ethanol (1 ml).

4.2.2.3 DTT [1 M]

A stock solution of DTT was prepared at the time of use by dissolving DTT powder (0.154 g) in dH_2O (500 µl). This solution was then made up to 2 ml with dH_2O and used in the thioredoxin activity assay.

4.2.2.4 NADPH [50 mM]

NADPH (10 mg) was stored in 1.5 ml microcentrifuge tubes at -20°C. Before use, dH_2O (250 µl) was added to a single tube. The stock solution was stored at-20°C.

4.3 Methods

4.3.1 Computational modeling

Kinetic parameter sets for the yeast thioredoxin system were obtained from the BRENDA database (Chang *et al.*, 2009), published literature and from our laboratory (Pillay *et al*., 2011) and were used to build the computational model in Python Simulator for Cellular System (PySCeS) (http://pysces.sourceforge.net). The system was modeled using realistic kinetic parameters and rate expressions (Pillay *et al.*, 2013). In the model, thioredoxin reductase was modeled with Michaelis-Menten kinetics, while IgY and insulin reduction reactions were described using mass action kinetics (Appendix 1) (Pillay *et al*., 2009).

In order to analyze the behavior of the system, a set of parameters and species concentrations resembling the *in vitro* reaction conditions (Table 4.1) were utilized and the data was plotted in double log space and linear space.

4.3.2 Isolation of immunoglobin Y (IgY)

The egg white and yolk were separated by carefully washing the egg yolk under running water. The yolk sac was punctured and yolk volume was determined in a measuring cylinder. The yolk sac was discarded and two volumes of 100 mM phosphate buffer, pH 7.6 containing 0.02% (w/v) sodium azide were added to the yolk and mixed thoroughly using a glass rod. A sample (50 µl) was taken at this stage and PEG (3.5% (w/v)) was added and mixed until the PEG had completely dissolved. The sample was centrifuged (4,420 × *g* for 20 min at room temperature). The supernatant was filtered through absorbent cotton wool which was placed at the base of a funnel noting that the filtrate must be a clear yellow liquid. If the

filtrate was not clear, the filtration step was repeated. The filtrate volume was recorded and another sample (50 µl) was removed. Thereafter, PEG concentration was increased to 12% and completely dissolved. The resulting mixture was centrifuged (12,000 × *g* for 10 min at room temperature) and a further sample (50 µl) was taken from the supernatant. The remaining supernatant was discarded and the pellet was dissolved in a volume of phosphate buffer equal to the original egg yolk volume. PEG was added to a final concentration of 12% (w/v) and the dissolved thoroughly. This mixture was then centrifuged (12,000 × *g* for 10 min at room temperature) and a sample (50 µl) was taken from the supernatant before discarding. The pellet was resuspended in phosphate buffer to a ⅙ of the original egg yolk volume and a final sample was taken and the purified IgY was then stored at -20^{o}C.

4.3.3 Thioredoxin activity

To determine the activity of our purified thioredoxin, the change in absorbance at 650 nm was directly monitored and the sample without the addition of the purified thioredoxin was used as the reference cuvette (blank). The reaction was initiated by the addition Trx (1.5 µM) to give a final volume of 1 ml for the reaction. The final reaction mixture contained insulin (0.01 mM), 63 mM potassium phosphate buffer (pH 7.0), EDTA (2 mM), Trx (1.5 µM) and DTT (1 mM). The absorbance measurements were recorded by the UV-1800 Shimadzu Spectrophotometer for 15 minutes following a 10 minute incubation period at 25^{o}C (Padayachee, 2013).

4.3.4 Thioredoxin reductase activity

The DTNB reducing activity of our purified thioredoxin reductase was determined in the presence of DTNB as a substrate by monitoring change in absorbance at 412 nm. This assay was done in the presence of univalent cations (NaCl) to increase the rate (Lim and Lim, 1995). The reaction mixture contained 0.1 M Tris-Cl (pH 8.0), 0.5 mM DTNB, 0.24 mM NADPH, 0.01% BSA and 0.5 M NaCl in a final volume of 1 ml. The reaction was started by the addition of the purified thioredoxin reductase (0.2 µM) and the change in absorbance was monitored at 412 nm. Absorbance measurements were recorded by the UV-1800 Shimadzu Spectrophotometer for 5 min at 25^{o}C.

Table 4.1 Species concentrations and kinetic parameters used in the model

Species	Value	References
NADPH	400 μM	This study
NADP	4 μM	This study
TrxSS	1.5 μM	This study
TrxSH	1.5 μM	This study
InsOx	10 μM	This study
InsRed	2 μM	This study
IgYOx	10μM	This study
IgYRed	2 μM	This study
Parameters	**Thioredoxin Reductase**	
[TR]	0.1 μM	This study
k_{cat}	43.7 s^{-1}	Oliveira *et al*., 2010
K_{nadph}	1.2 μM	Williams, 1976
K_{trxss}	2.8 μM	Williams, 1976
k_2	1 $\mu M^{-1}s^{-1}$	Estimated
k_3	1 $\mu M^{-1}s^{-1}$	Estimated

4.3.5 IgY reduction by thioredoxin

To prove that thioredoxin can reduce IgY disulfide bonds we used the thioredoxin activity assay (Holmgren, 1979). In this assay, the reaction mixture contained 2 mM EDTA, 100 mM potassium phosphate buffer (pH 7.0), 0.4 mM NADPH, 1.5 μM thioredoxin, thioredoxin reductase (0.1 μM) and IgY (10 μM) to the final volume of 0.5 ml. The reaction was initiated by the addition of IgY and the rate of NADPH oxidation was measured by the decrease in absorbance at 340 nm by the UV-1800 Shimadzu Spectrophotometer for

5 minutes. A sample without the addition of IgY was used as the reference cuvette (blank). As a control experiment, to verify that the reduction of IgY disulfide bonds would not cause interference in the kinetic analysis of the thioredoxin activity assay (Section 4.3.3), the absorbance at 650 nm was also monitored. In this experiment, the reaction mixture contained IgY (0.01 mM), 63 mM potassium phosphate buffer (pH 7.0), EDTA (2 mM), Trx (1.5 μM) and DTT (1 mM) in a final volume of 0.5 ml. The reaction was also initiated by the addition of IgY and the change in absorbance was measured at 650 nm by the UV-1800 Shimadzu Spectrophotometer for 5 minutes. Similarly, a sample without the addition IgY was used as the reference cuvette (blank).

4.3.6 Competition assay

In the competition assay (Fig. 4.2), IgY was expected to act as a competitive substrate for thioredoxin. The rate of NADPH consumption for insulin (control experiment) and IgY reduction were followed at 650 nm by the UV-1800 Shimadzu Spectrophotometer for 5 min at 25^{o}C. The reaction mixture contained 2 mM EDTA, 100 mM potassium phosphate buffer (pH 7.0), 0.4 mM NADPH, 1.5 μM thioredoxin, insulin (10 μM), IgY (0-30 μM) and thioredoxin reductase (0.1 μM) in a final volume of 0.5 ml. As a positive control in the experiment, to verify that components such as the buffer, NADPH, Trx and thioredoxin reductase were functional, insulin (10 μM) was used as the only substrate and a reference cuvette without the addition of any substrate (IgY/Insulin) was used as the blank.

4.4 Results

4.4.1 Computational modeling

The yeast thioredoxin system was computationally modeled (Appendix 1) in order to study the interconnectivity between thioredoxin-dependent reactions. To analyze this system, IgY was varied and the effect of this change on the fluxes through the thioredoxin system was determined and plotted below. The computational data showed that the steady state flux of insulin reduction and that of IgY reduction affected each other (Fig. 4.3). For a given insulin concentration, the addition of IgY to the system at 10 μM (red), 20 μM (blue) and 30 μM (green), reduced the flux of the insulin reduction reaction (Fig. 4.3 A and B) in a concentration-dependent manner.

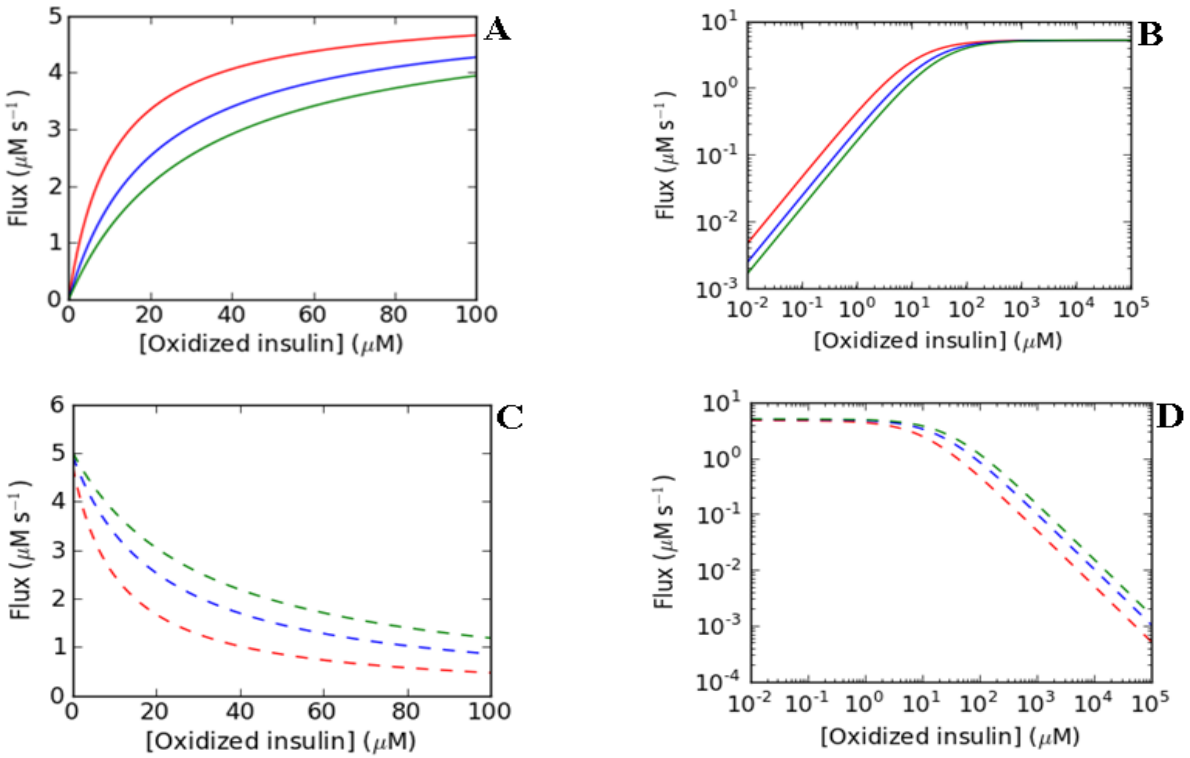

Figure 4.3 Thioredoxin-dependent reactions can affect each other. In each of these simulations, the steady state flux of the thioredoxin-dependent reduction of insulin at varying concentrations (IgY) is shown. IgY was varied from 10 µM (red), 20 µM (blue) and 30 µM (green). The steady state fluxes of insulin reduction (A and B) and IgY reduction (C and D) were monitored. Fig. 4.3 A and C were plotted in linear space while Fig. 4.3 B and D were plotted in double log space to show scaled changes in the flux (Pillay *et al*., 2013).

At higher concentrations of insulin, the IgY was outcompeted and the reactions approached the same limiting rate. Similarly, an increase in insulin concentration decreased the flux of the IgY reduction reaction (Fig. 4.3 C and D).

4.4.2 *In vitro* analysis

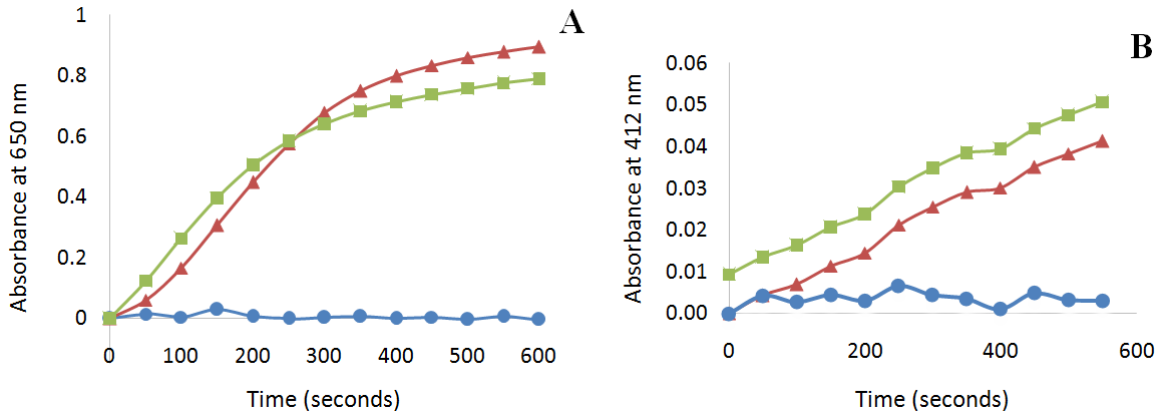

Figure 4.4 Confirming the activity of the purified thioredoxin and thioredoxin reductase. A) typical turbidimetric curves upon addition of *S. cerevisiae* thioredoxin (1.5 µM) are shown, in comparison to turbidity formed in the no thioredoxin control with addition of DTT only (blue). In B) the colorimetric linear relationship between absorbance at 412 nm and time, for the reduction of DTNB (0.5 mM) by *S. cerevisiae* thioredoxin reductase (0.2 µM) are shown, in comparison to the color change upon exclusion of thioredoxin reductase in the reaction mix (blue). Experiments were performed in duplicate.

A thioredoxin activity assay was utilized to confirm activity of the purified thioredoxin by the change in absorbance at 650 nm (Holmgren, 1979). It was evident from the rates of insulin reduction obtained (7.5×10^{-5} ΔA_{650}/min) that the purified thioredoxin samples were active. The reduction of DTNB was used to measure the purified thioredoxin reductase activity by the change in absorbance at 412 nm (Lim and Lim, 1995). It was also evident by the rates of DTNB reduction obtained (2.33×10^{-3} ΔA_{412}/min) that the purified thioredoxin reductase was active.

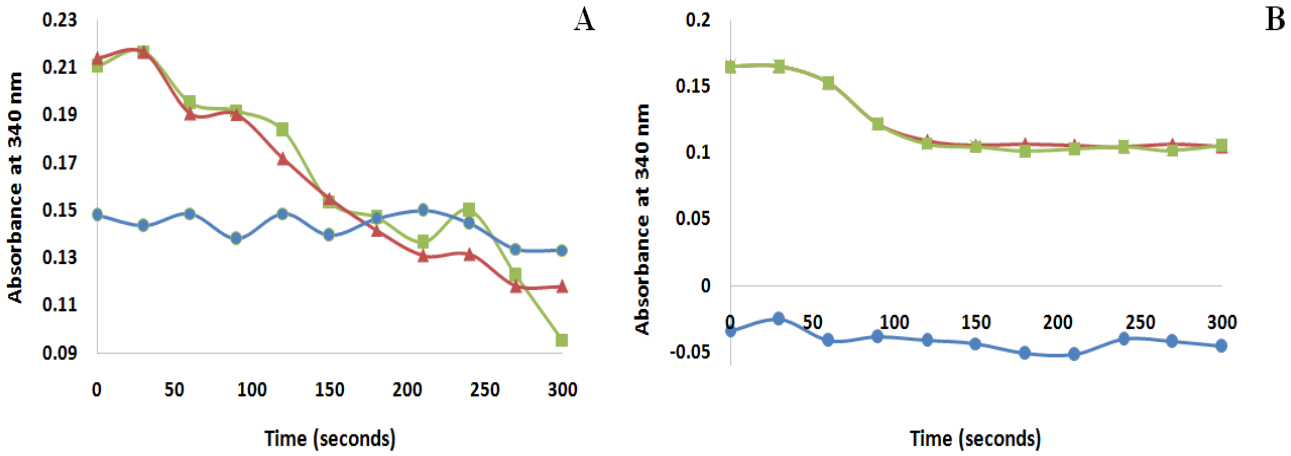

Figure 4.5 IgY was a substrate for the thioredoxin system. As a positive control A) NADPH consumption was determined by the decrease of absorbance at 340 nm during the initial linear phase as insulin (10 µM) was reduced (red and green) using the sample without addition of insulin as a control (blue). In B) NADPH consumption was also determined from the decrease in absorbance at 340 nm as IgY was reduced (red and green) using the sample without addition IgY (10 µM) as a control (blue). Experiments were performed in duplicate and proceeded at 25°C.

The next step was to prove that IgY could be used as a substrate for thioredoxin. As a positive control, insulin reduction by the thioredoxin system was carried out. The rate of NADPH oxidation was measured and found to be $6.50 \times 10^{-4} \pm 0.01$ ΔA_{340}/min (Table 4.2). Similarly, to test NADPH oxidation using IgY as a substrate, the same experiment was undertaken using IgY as a substrate and the data indicated that IgY disulfides were rapidly reduced causing the reaction to stop after 100 seconds (Fig. 4.5 B). Evidently, IgY could be used as a substrate of the thioredoxin system as the rate of NADPH oxidation was found to be in the same range as insulin (Table 4.2).

Table 4.2 Comparison of the rates of NADPH oxidation using insulin and IgY as substrates

Substrate	Rate (A_{340}/min)	Standard error	Percentage error
Insulin (10 µM)	6.50×10^{-4}	0.01	6.14
Immunoglobin Y (10 µM)	5.10×10^{-4}	0.01	8.20

To ensure that IgY reduction by thioredoxin would not cause interference in the insulin turbidity assay at 650 nm, we analysed the reduction of IgY catalysed by thioredoxin.

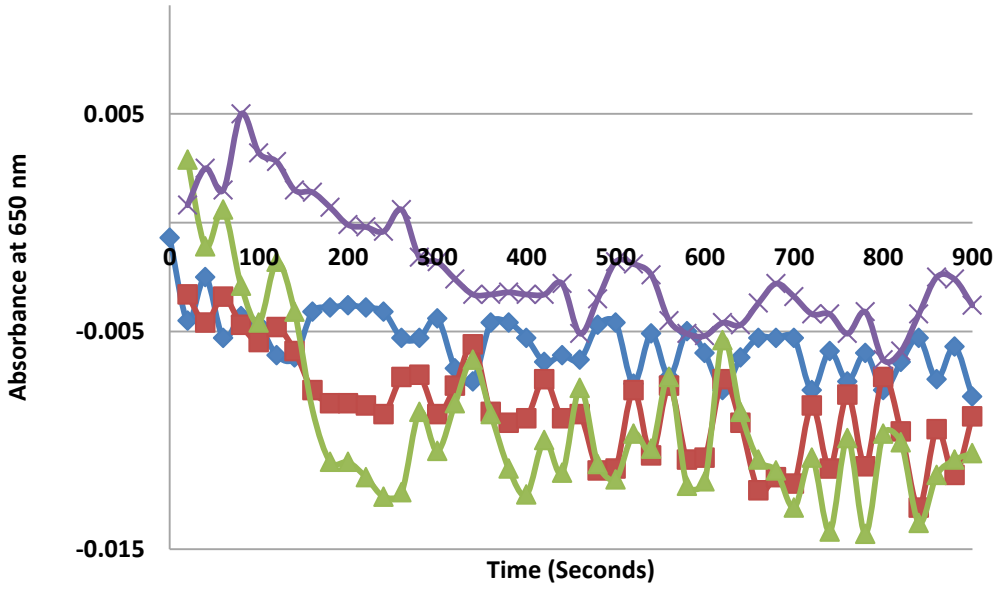

Figure 4.6 IgY reduction does not affect the absorbance at 650 nm. A turbidimetric assay upon addition of *S. cerevisiae* thioredoxin (1.5 µM) with varying IgY concentrations (10 µM purple; 20 µM green; 30 µM red) was compared to a reaction mixture without IgY (blue).

There was no change of absorbance at 650 nm with 1.5 µM thioredoxin and 1 mM DTT at pH 7.0 over increasing IgY concentrations (0 - 30 µM). Thus, IgY in its oxidized or reduced form does not absorb significantly at 650 nm therefore we expected that if the competition assay was monitored at this wavelength, it would be specific for insulin.

In order to investigate the behaviour of the thioredoxin system with two substrates, the rate of insulin precipitation in the presence of IgY was monitored at 650 nm. As a control, the rate of reduction by the thioredoxin system with insulin alone was monitored and was not affected in these assays (Fig. 4.7 A-D (red)). Different concentrations of IgY where tested in duplicate in this assay at 10 µM (Fig. 4.7 A), 20 µM (Fig. 4.7 B) and 30 µM (Fig. 4.7 C) (green and purple). These results were then combined into a single figure (Fig. 4.7 D).

The initial rates were then analysed and one was found to be different within the initial phase of the assay. The rates with 10 µM and 30 µM of IgY showed a 10-fold change while the 20 µM IgY reaction mixture showed no change from the reaction with insulin only (Table 4.3). However, the reaction with 20 µM IgY had the highest rate of all the IgY containing reactions (10 µM and 30 µM). These enigmatic results suggest the requirement of more replications in the assay. Further, although there appeared to be a difference in initial rates, an additional pattern was observed in the assay. Following the expected linear increase in precipitation, a concentration-dependent decrease in absorbance was observed. Thus, the more IgY was added to the assay, the faster the precipitation occurred thus resulting in the decrease in absorbance at 650 nm (Fig. 4.7 D). This was an unexpected result and suggested a possible interaction between the substrates in the system.

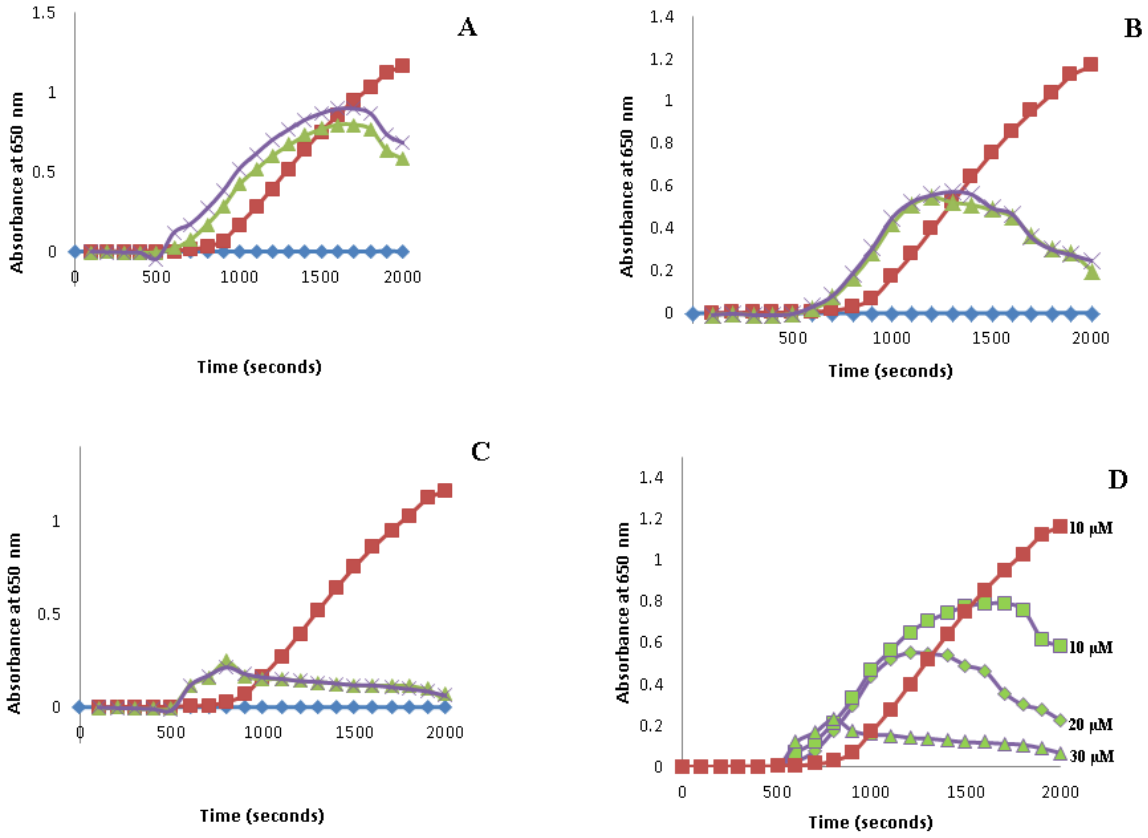

Figure 4.7 Competition assay for thioredoxin reduction. In each of these graphs the reaction of thioredoxin reduction of the substrate insulin (red) at varying concentrations of IgY is shown. Duplicate IgY-Insulin assays at varying IgY concentrations from 10 µM (A), 20 µM (B) and 30 µM (C) (green and purple) were performed with a no substrate blank (blue) included. In D) an overall presentation of the competition assay is shown at 25°C and was monitored at 650 nm.

Additionally, a *t-test* was performed to analyse if there is a significant difference in rates when IgY concentration was increased. The critical level was set at 0.05 (critical *p*-value) and the change in rates for 10 µM and 20 µM IgY were found to be insignificant as *t* was bigger than 0.05 for both concentrations (Table 4.3). However, the change was found to be statistically significant for the 30 µM IgY sample as *t* was found to be smaller than 0.05 (Table 4.3). These statistical results also suggested the need for more replications in the competition assay.

Table 4.3 Comparison of the rates of NADPH oxidation using insulin and insulin and/IgY as substrates and statistical significance caused by addition of IgY

Substrates	**Rate (ΔA_{650}/min)**	**Rate (ΔA_{650}/min)**	**Rate (ΔA_{650}/min)**
Immunoglobin Y	**10 µM**	**20 µM**	**30 µM**
Insulin	1.00×10^{-3}	1.00×10^{-3}	1.00×10^{-3}
Insulin and IgY	$9.40 \pm 0.02 \times 10^{-4}$	$1.10 \pm 0.05 \times 10^{-3}$	$4.90 \pm 0.07 \times 10^{-4}$
***t-test* (critical *p*-value = 0.05)**			
Immunoglobin Y	**10 µM**	**20 µM**	**30 µM**
t Stat	-0.060	1.244	2.987
P(T<=t) one-tail	0.476	0.112	0.004
P(T<=t) two-tail	0.953	0.223	0.007

4.5 Discussion

An assay based on the DTT-dependent reduction of insulin by thioredoxin was used to determine the activity of the purified thioredoxin (Holmgren, 1979b). While, the activity of thioredoxin reductase was assayed using 5,5'-dithiobis-2-nitrobenzoic acid (DTNB). This assay enabled the examination of the activity purified thioredoxin reductase in the absence of thioredoxin. Lim and Lim (1995) showed that the use of univalent cations such as sodium

chloride in the thioredoxin reductase activity assay significantly increased the rate of reduction of DTNB. Once it was confirmed that the purified thioredoxin and thioredoxin reductase were active (Fig. 4.3), the next step involved analysis of the system with two substrates first computationally and *in vitro* by a novel competition assay.

Our computational modelling analysis confirmed that an increase in concentration of one of the substrates in the thioredoxin system decreased the flux of another thioredoxin oxidation reaction (Fig. 4.3). In our *in vitro* analysis, we used the standard insulin reduction assay for thioredoxin activity with two substrates (IgY and insulin). Our results showed that an increase in one substrate concentration could affect the rate of another thioredoxin oxidation reaction at higher concentrations of IgY (Table 4.3). However, the results were enigmatic as an increase in IgY concentration resulted in an unexpected decrease in absorbance at 650 nm (Fig. 4.6 D). This result could have been due to the exceptional rate of IgY reduction (Fig. 4.4 B) and the possible interaction between the two substrates in the assay (below).

IgY reduction by the thioredoxin system occurred rapidly within the first 100 seconds as measured by NADPH oxidation (Fig. 4.4 B), before turbidity was visible in the 650 nm assay (Fig. 4.6). Thus, it is possible that the statistically weak effects of IgY on the rate of insulin reduction (Table 4.3) could be due to the fact that IgY was already reduced completely. Therefore, the use of a higher IgY concentration would be recommended for a more accurate analysis of the competition assay as there would still be IgY available to be reduced after the first 100 seconds of the assay. The unexpected decrease in absorbance observed in this assay could be due to IgY increasing the rate of insulin precipitation. This effect was previously demonstrated in experiments by Cantrell *et al*. (1972) who showed that a polymer of denatured insulin is formed which is capable of binding to IgG (immunoglobulin similar to IgY) in a way that produces a complement-fixing aggregation of IgG. Although the chemical nature of this insulin-IgG interaction is unknown, the partial dissociation observed with immunoelectrophoresis following solubilization suggested a non-covalent interaction (Cantrell *et al*., 1972). These results showed that the precipitate composition was approximately 80% insulin and 20% IgG which emphasized that IgG was a co-precipitant of insulin and our data also suggests that IgY is a potent insulin co-precipitant.

Several investigators found that complexes of insulin and IgG were formed when exogenous insulin was administered to patients with anti-insulin antibodies (Abrass *et al*.,

1983). These complexes of insulin and IgG contributed to an increased load of circulating immune complexes in patients with diabetes mellitus and offered a possible explanation for the presence of these components in microangiopathic lesions and may be a contributing factor to the pathogenesis of diabetic microangiopathy (Farquhar and Palade, 1962). Interestingly, insulin aggregation has been previously investigated. The proposed mechanism included insulin's self-association into dimers and hexamers, the interactions with hydrophobic surfaces and formation of stable intermediate species which could interact with other present molecules (Jeffrey *et al*., 1976). Insulin aggregation is observed under conditions such as neutral pH, mild agitation, slightly elevated temperature (which are similar to conditions in the competition assay) and mild reducing conditions which lead to denaturation and precipitation (Brange *et al*., 1987). This was subsequently accompanied by exposure of hydrophobic groups resulting in unstable conformations which seek to minimize their surface energy by interacting with other unfolded molecules (Joly, 1965). This phenomenon could explain the possible interaction between the two substrates in the assay leading to rapid precipitation followed by a decrease in absorbency at 650 nm. Collectively, our analysis showed that there was a complex interaction between thioredoxin oxidation reactions, suggesting that our competition assay requires improvement, especially with respect to IgY concentration and more replications. In addition, the use of a different thioredoxin substrate could also be of consideration.

Chapter 5: GENERAL DISCUSSION

The thioredoxin system is essential for maintaining the cellular redox status and plays an important role in a variety of cellular functions (Toledano *et al*., 2007). However, elevated levels of this system have been associated with certain diseases including HIV, malaria and cancer. Therefore it is evident that the construction of kinetic models is necessary to understand how complex networks such as the thioredoxin system can be regulated (Pillay *et al.*, 2013). Hence computational modeling approaches were used in this study to develop a model of the yeast thioredoxin system to investigate the connectivity in thioredoxin oxidation reactions. To confirm the *in silico* analysis, *in vitro* kinetic analyses were planned using a novel competition assay. In order to achieve this, yeast thioredoxin and thioredoxin reductase needed to be cloned, expressed and purified (Chapter 3).

The thioredoxin system was isolated from *S. cerevisiae*, cloned and expressed in *E. coli* and subsequently purified using nickel affinity-chromatography (Chapter 3). *S. cerevisiae* was chosen to study the thioredoxin system due to its ability to be genetically and biochemically manipulated and the availability of mutants lacking components of the system (Grant, 2001, Wheeler and Grant, 2004). Thus the *in vitro* results obtained in this study could be followed up *in vivo.*

As a first step, it was important to make use of cheap activity assays for both thioredoxin and thioredoxin reductase that did not require the use of its counterpart. In order to detect the activity of thioredoxin reductase, an assay utilizing univalent cations in the reaction mixture to increase the rate of DTNB reduction by thioredoxin reductase was chosen (Lim and Lim, 1995). To detect thioredoxin activity, the DTT-dependent reduction of insulin was utilized (Chapter 4). The use of DTT, instead of thioredoxin reductase and the inclusion of a preincubation step to reduce thioredoxin with DTT, made this assay substantially cheaper (Padayachee, 2013).

Computational modeling was used to study interconnectivity between thioredoxin-dependent reactions by varying IgY and analyzing the effect of this change on the fluxes through the thioredoxin system. These results showed that the steady state flux of insulin reduction should be affected by increases in the IgY concentration in a concentration-dependent manner (Chapter 4). To confirm these computational findings, *in vitro* kinetic analyses were undertaken using the insulin assay (Holmgren, 1979). Through these analyses,

a number of technical goals were achieved. This study showed that IgY can be used as a substrate for thioredoxin and this was demonstrated by the apparent NADPH oxidation at 340 nm with IgY (Fig. 4.4 B). Furthermore, IgY was an excellent substrate as its reduction reaction proceeded at a comparable rate to that of insulin (Table 4.2). In our assays, the thioredoxin dependent reduction of IgY was complete in 100 seconds (Fig. 4.5 B) compared to insulin reduction that still proceeded beyond 100 seconds (Fig. 4.5 A).

However, our *in vitro* kinetic analyses results were not completely convincing. Although IgY appeared to be a thioredoxin substrate there were some complications in the competition assay. IgY concentrations of 10-20 μM had contradictory or small effects on the rate on insulin reduction. However at 30 μM IgY, a significant decrease in the rate of insulin reduction was observed. These results suggested that the IgY could have been completely reduced before insulin aggregation was detected at 650 nm. Furthermore, this reduction of IgY appeared to enhance insulin aggregation which increased the rate of precipitation and thus decreased the absorbency at 650 nm. These unexpected results suggest that a higher concentration of IgY is required in order to further analyse competing thioredoxin substrates *in vitro*. Alternatively, substrates such as ribonuclease, peroxiredoxin, or aconitase B could be tested as competing substrates in this assay. An advantage of using these substrates is that their activity could be measured as well (Yamazaki *et al*., 2004).

In summary, these findings serve as an important starting point in the understanding of how thioredoxin-dependent reactions are connected to one another and how this connection affects regulation within the system. Further, this work may force a rethink about drugs that target the thioredoxin system as competing effects may change the active concentration of inhibitors needed for effective therapy. Hopefully, the development of smarter and more effective drug design strategies could lead to significant advances in the treatment of pathologies where the thioredoxin system has been implicated.

References

ABRASS, C. K., HEBER, D. & LIEBERMAN, J. 1983. Circulating immune complexes in patients with diabetes mellitus. Clinical and Experimental Immunology, 52, 164–172.

ADELEKAN, D. & THURNHAM, D. 1998. Glutathione peroxidase (EC 1.11.1.9) and superoxide dismutase (EC 1.15.1.1) activities in riboflavin-deficient rats infected with Plasmodium berghei malaria. *The British Journal of Nutrition,* 79, 305-309.

ARNÉR, E. S. J. & HOLMGREN, A. 2000a. Physiological functions of thioredoxin and thioredoxin reductase. *European Journal of Biochemistry,* 267, 6102-6109.

ARNÉR, E. S. J. & HOLMGREN, A. 2000b. Measurement of Thioredoxin and Thioredoxin Reductase. *Current Protocols in Toxicology*.

ARNÉR, E. S. J. & HOLMGREN, A. 2006. The thioredoxin system in cancer. *Seminars in Cancer Biology,* 16, 420-426.

BENOV, L. & AL-IBRAHEEM, J. 2002. Disrupting *Escherichia coli*: A Comparison of Methods. *Journal of Biochemistry and Molecular Biology,* 35, 428-431.

BRADFORD, M. M. 1976. A rapid and sensitive method for the quantitation of microgram quantities of protein utilizing the principle of protein-dye binding. *Analytical Biochemistry,* 72, 248-254.

BRANGE, J., HANSEN, J. F., HAVELUND, S. & MELBERG, S. G. 1987. *Studies of the insulin fibrillation process, in: Advanced Models for the Therapy of Insulin-Dependent Diabetes*, New York, Raven Press.

BUCHANAN, B. B., HOLMGREN, A., JACQUOT, J. P. & SCHEIBE, R. 2012. Fifty years in the thioredoxin field and a bountiful harvest. *Biochimica et Biophysica Acta (BBA) - General Subjects,* 1820, 1822-1829.

CANTRELL, J. W., STROUND, R. M. & PRUITT, K. M. 1972. Insulin and IgG complexes: An immunologic bypass for complement activation. *Diabetes*, 21, 872-880.

CHA, M. K., SUH, K. H & KIM, I. H. 2009. Overexpression of peroxiredoxin I and thioredoxin1 in human breast carcinoma. *Journal of Experimental & Clinical Cancer Research,* 28, 93.

CHANG, A., SCHEER, M., GROTE, A., SCHOMBURG, I. & SCHOMBURG, D. 2009. BRENDA, AMENDA and FRENDA the enzyme information system. *Nucleic Acids Research,* 37, 588-592.

COMPTON, S. J. & JONES, C. G. 1985. Mechanism of dye response and interference in the Bradford protein assay. *Analytical Biochemistry*, 151, 369-374.

D'ALESSANDRO, A., RINALDUCCI, S. & ZOLLA, L. 2011. Redox proteomics and drug development. *Journal of Proteomics,* 74, 2575-2595.

DENNISON, C. 2003. *A Guide to Protein Isolation,* Netherlands, Kluwer academic publishers.

DRACULIC, T., DAWES, I. & GRANT, C. 2000. A single glutaredoxin or thioredoxin is essential for viability in the yeast *Saccharomyces cerevisiae. Molecular Microbiology,* 36, 1167-1174.

FARQUHAR, M. G & PALADE, E. E. 1962. Functional evidence for the existence of a third cell type in the renal glomerulus. *Journal of Cell Biology*, 13, 55-87

GAN, Z. 1991. Yeast thioredoxin genes. *Journal of Biological Chemistry,* 266, 1692-1696.

GARRIDO, E. O. & GRANT, C. M. 2002. Role of thioredoxins in the response of *Saccharomyces cerevisiae* to oxidative stress induced by hydroperoxides. *Molecular Microbiology*, 43, 993–1003.

GILBERT, S. 2010. *Developmental Biology,* Minnesota, Sinauer Associates.

GRANT, C. M. 2001. Role of the glutathione/glutaredoxin and thioredoxin systems in yeast growth and response to stress conditions. *Molecular Microbiology,* 39, 533-541.

GROGAN, T., FENOGLIO-PRIESER, C., ZEHEB, R., BELLAMY, W., FRUTIGER, Y., VELA, E., STEMMERMAN, G., MACDONALD, J., RICHTER, L., GALLEGOS, A. & POWIS, G. 2000. Thioredoxin, a putative oncogene product, is overexpressed in

gastric carcinoma and associated with increased proliferation and increased cell survival. *Human Pathology,* 31, 475–481.

GROMER, S., URIG, S. & BECKER, K. 2004. The thioredoxin system-from science to clinic. *Medical Care Research and Review,* 24, 40-89.

HALL, D., BALDESTEN, A., HOLMGREN, A. & REICHARD, P. 1971. Yeast Thioredoxin. *European Journal of Biochemistry,* 23, 328-335.

HAN, H., BEARSS, D. J., BROWNE, L. W., CALALUCE, R., NAGLE, R. B. & VON HOFF, D. D. 2002. Identification of differentially expressed genes in pancreatic cancer cells using cDNA microarray. *The Journal of Cancer Research,* 62, 2860-2896.

HARJU, S., FEDOSYUK, H. & PETERSON, K. 2004. Rapid isolation of yeast genomic DNA: Bust n' Grab. BMC Biotechnology, 4, 8.

HARMS, C., MEYER, M. & ANDREESEN, J. 1998. Fast purification of thioredoxin reductases and of thioredoxins with an unusual redox-active centre from anaerobic, amino-acid-utilizing bacteria. *Journal of Microbiology*, 144, 793-800.

HEDLEY, D., PINTILIE, M., WOO, J., NICKLEE, T., MORRISON, A., BIRLE, D., FYLES, A., MILOSEVI, C. M. & HILL, R. 2004. Up-regulation of the redox mediators thioredoxin and apurinic/apyrimidinic excision (APE)/Ref-1 in hypoxic microregions of invasive cervical carcinomas, mapped using multispectral, wide-field fluorescence image analysis. *American Journal of Pathology,* 164, 557–565.

HOLMGREN, A. & LU, J. 2010. Thioredoxin and thioredoxin reductase: Current research with special reference to human disease. *Biochemical and Biophysical Research Communications,* 396, 120-124.

HOLMGREN, A. 1968. Thioredoxin 6: The amino acid sequence of the protein from Escherichia coli B. *European Journal of Biochemistry,* 6, 475–484.

HOLMGREN, A. 1979. Reduction of disulfides by thioredoxin. Exceptional reactivity of insulin and suggested functions of thioredoxin in mechanism of hormone action. *Journal of Biological Chemistry,* 254, 9113-9119

HOLMGREN, A. 1979. Thioredoxin catalyzes the reduction of insulin disulfides by dithiothreitol and dihydrolipoamide. *Journal of Biological Chemistry,* 254, 9627-9632.

HOLMGREN, A. 1985. Thioredoxin. *Annual Review of Biochemistry,* 54, 237-271.

INOUE, Y., NOMURA, W., TAKEUCHI, Y., OHDATE, T., TAMASU, S., KITAOKA, A., KIYOKAWA, Y., MASUTANI, H., MURATA, K., WAKAI, Y., IZAWA, S. & YODOI, J. 2007. Efficient extraction of thioredoxin from *Saccharomyces cerevisiae* by ethanol. *Applied and Environmental Microbiology,* 73, 1672-1675.

IWAO-KOIZUMI, K., MATOBA, R., UENO, N., KIM, S., ANDO, A., MIYOSHI, Y., MAEDA, E., NOGUCHI, S. & KATO, K. 2005. Prediction of docetaxel response in human breast cancer by gene expression profiling. *Journal of Clinical Oncology,* 23, 422–431.

JEFFREY, P. D., MILTHORPE, B. K. & NICHOL, L. W. 1976. Polymerization Pattern of Insulin at pH 7.0. *Biochemistry*, 15, 4660-4665.

JOLY, M. 1965. A physiochemical approach to the denaturation of proteins. Molecular biology; an international series of monographs and textbooks. London, Academic Press.

JONES, D. P. 2010. Redox sensing: orthogonal control in cell cycle and apoptosis signalling. *Journal of Internal Medicine,* 268, 432-448.

KARLENIUS, T. C. & TONISSEN, K. F. 2010. Thioredoxin and Cancer: A Role for Thioredoxin in all States of Tumor Oxygenation. *Cancers,* 2, 209-232.

KEMP, M., GO, Y. M. & JONES, D. P. 2008. Nonequilibrium thermodynamics of thiol/disulfide redox systems: A perspective on redox systems biology. *Free Radical Biology and Medicine,* 44, 921-937.

KIM, H., CHAE, H., KIM, Y., KIM, Y., HWANGS, T., PARK, E. & PARK, Y. 2003. Preferential elevation of Prx I and Trx expression in lung cancer cells following hypoxia and in human lung cancer tissues. *Cell Biology and Toxicology,* 19, 285–298.

KIM, J. A., PARK, S., KIM, K., RHEEC, S. G. & KANG, S. W. 2005. Activity assay of mammalian 2-cys peroxiredoxins using yeast thioredoxin reductase system. *Analytical Biochemistry,* 338, 216-223.

KONCAREVIC, S., ROHRBACH, P., DEPONTE, M., KROHNE, G., PRIETO, J. H., III, J. Y., RAHLFS, S. & BECKER, K. 2009. The malarial parasite Plasmodium falciparum imports the human protein peroxiredoxin 2 for peroxide detoxification. *PNAS Journal,* 106, 13323-13328.

KRAUTH-SIEGEL, R. L. & COMINI, M. A. 2008. Redox control in trypanosomatids, parasitic protozoa with trypanothione-based thiol metabolism. *Biochimica et Biophysica Acta (BBA) - Proteins and Proteomics,* 1780, 1236-1248.

KURIYAN, J., KRISHNA, T., WONG, L., GUENTHER, B., PAHLER, A., WILLIAMS, C. J. & MODEL, P. 1991. Convergent evolution of similar function in two structurally divergent enzymes. *Nature,* 352, 172–174.

LAURENT, T., MOORE, E. & REICHARD, P. 1964. Enzymatic synthesis of deoxyribonucleotides. IV. Isolation and characterization of thioredoxin, the hydrogen donor from Escherichia coli B. *Journal of Biological Chemistry,* 239, 3436–3444.

LESLIE, G. A. & CLEM, L. W. 1969. Phylogeny of Immunoglobulin Structure and Function. III. Immunoglobulins of the Chicken. *Journal of Experimental Medicine*, 130, 1337-1352.

LIM, H. W. & LIM, C. J. 1995. Direct reduction of DTNB by *E. coli* thioredoxin reductase. *Journal of Biochemistry and Molecular Biology,* 28, 17-20.

LIPPOLDT, A., PADILLA, C. A., GERST, H., ANDBJER, B., RICHTER. E., HOLMGREN, A. & FUXE, K. 1995. Localization of thioredoxin in the rat brain and functional implications. *Journal of Neuroscience*, 15, 6747–6756.

LU, J. & HOLMGREN, A. 2012. The thioredoxin antioxidant system. *Antioxidants & Redox Signaling*, 17, 1738-1747.

LUIKENHUIS, S., DAWES, W. & GRANT, C. 1997. The yeast *Saccharomyces cerevisiae* contains two glutaredoxin genes that are required for protection against reactive oxygen species. *Molecular Biology of the Cell*, 9, 1081-1091.

LUKOSZ, M., JAKOB, S., BUCHNER, N., ZSCHAUER, T. C., ALTSCHMIED, J. & HAENDELER, J. 2010. Nuclear redox signaling. *Antioxidants and redox signaling,* 12, 713-742.

MAHMOOD, D. F., ABDERRAZAK, A., KHADIJA, E. H., SIMMET, T. & ROUIS, M. 2013. The Thioredoxin System as a Therapeutic Target in Human Health and Disease. *Antioxidants and Redox Signalling*, 26, 398-404.

MARKS, P. 2006. Thioredoxin in cancer--role of histone deacetylase inhibitors. *Seminars in Cancer Biology,* 16, 436-4443.

MIRANDA-VIZUETE, A., DAMDIMOPOULOS, A. E., GUSTAFSSON, J. A. & SPYROU, G. 1997. Cloning, Expression, and Characterization of a Novel Escherichia coli Thioredoxin. *The Journal of Biological Chemistry,* 272, 30841–30847.

MIYAZAKI, K., NODA, N., OKADA, S., HAGIWARA, Y., MIYATA, M., SAKURABAYA, I., YAMAGUCHI, N., SUGIMURA, T., TERADA, M. & WAGASUGI, H. 1998. EIevated serum level of Thioredoxin in patients with Hepatocellular Carcinoma. *Biotheraphy*, 11, 277-288.

MOORE, E., REICHARD, P. & THELANDER, L. 1964. Enzymatic Synthesis of Deoxyribonucleotides. V. Purification and properties of thioredoxin reductase from *Escherichia coli B*. *Journal of Biological Chemistry,* 239, 3445-3452.

MULLER, E. G. D. 1996. A glutathione reductase mutant of yeast accumulates high levels of oxidized glutathione and requires thioredoxin for growth. *Molecular Biology of the Cell*, 7, 1805–1813.

MULLER, E.G. D. 1991. Thioredoxin deficiency in yeast prolongs S phase and shortens the G1 interval of the cell cycle. *Journal of Biological Chemistry,* 266, 9194-9202.

MUSTACICH, D. & POWIS, G. 2000. Thioredoxin reductase. *Biochemistry,* 346, 1-8.

NAKAMURA, H., DE ROSA, S. C., YODOI, J., HOLMGREN, A., GHEZZII, P., HERZENBERG, L. A. & HERZENBERG, L. A. 2001. Chronic elevation of plasma thioredoxin: Inhibition of chemotaxis and curtailment of life expectancy in AIDS. *PNAS*, 98, 2688–2693.

NAKAMURA, H., DE ROSA, S., ROEDERER, M., ANDERSON, M., DUBS, J., YODO, I. J., HOLMGREN, A. & HERZENBERG, L. 1996. Elevation of plasma thioredoxin levels in HIV-infected individuals. *International Immunology,* 8, 603-611.

NEWMAN, G., BALCEWICZ-SABLINSKA, M., GUARNACCIA, J., REMOLD, H. & SILBERSTEIN, D. 1994. Opposing regulatory effects of thioredoxin and eosinophil cytotoxicity-enhancing factor on the development of human immunodeficiency virus 1. *Journal of Experimental Medicine,* 180, 359–363.

NICKEL, C., RAHLFS, S., DEPONTE, M., KONCAREVIC, S. & BECKER, K. 2006. Thioredoxin networks in the malaria parasite Plasmodium falciparum. *Antioxidants and Redox Signaling,* 8, 1227-1239.

OLIVEIRA, M. A., DISCOLA, K. F., ALVES, S. V., MEDRANO, F. J., GUIMARAES, B. G. & NETTO, L. E. S. 2010. Insights into the Specificity of Thioredoxin Reductase-Thioredoxin Interactions. A Structural and Functional Investigation of the Yeast Thioredoxin System. *Biochemistry,* 49, 3317-3326.

PACE, G. & LEAF, C. 1995. The role of oxidative stress in HIV disease. *Free Radical Biology and Medicine,* 19, 523-528.

PADAYACHEE, L. 2013. Regulation of the thioredoxin system in *Saccharomyces cerevisiae*. MSc thesis. University of Kwa-Zulu Natal.

PEDRAJAS, J., KOSMIDOU, E., MIRANDA-VIZUETE, A., GUSTAFSSON, J., WRIGHT, A. & SPYROU, G. 1999. Identification and functional characterization of a novel mitochondrial thioredoxin system in *Saccharomyces cerevisiae*. *Journal of Biological Chemistry,* 274, 6366-6373.

PERRONE, G., TAN, S. & DAWES, I. 2008. Reactive oxygen species and yeast apoptosis. *Biochimica et Biophysica Acta (BBA) - Proteins and Proteomics,* 1783, 1354–1368.

PILLAY, C. S., HOFMEYR, J. H. S., MASHAMAITE, L. N. & ROHWER, J. M. 2013. From Top-Down to Bottom-Up: Computational Modeling Approaches for Cellular Redoxin Networks. *Antioxidants and redox signaling*, 18, 2075-2086.

PILLAY, C., HOFMEYR, J. & ROHWER, J. 2011. The logic of kinetic regulation in the thioredoxin system. *BMC Systems Biology,* 5, 1-15.

PILLAY, C., HOFMEYR, J., OLIVIER, B., SNOEP, J. & ROHWER, J. 2009. Enzymes or redox couples? The kinetics of thioredoxin and glutaredoxin reactions in a systems biology context. *Biochemistry,* 417, 269-275.

PORQUÉ, P. G., BALDESTEN, A. & REICHARD, P. 1970. Purification of a Thioredoxin System from Yeast. *The Journal of Biological Chemistry,* 245, 2363-2370.

PÜRZEL, J., SCHMITT, R., VIERTLBOECK, B.C. & GÖBEL, T.W. 2009. Chicken IgY binds its receptor at the CH3/CH4 interface similarly as the human IgA: Fc alpha RI interaction. *Journal of Immunology*, 183, 4554–4559.

RAFFEL, J., BHATTACHARYYA, A., GALLEGOS, A., CUI, H., EINSPAHR, J., ALBERTS, D. & POWIS, G. 2003. Increased expression of thioredoxin-1 in human colorectal cancer is associated with decreased patient survival. *Journal of Laboratory and Clinical Medicine,* 142, 46–51.

REECE, R. J. 2004. *Analysis of Genes and Genomes,* England, John Wiley and Sons Ltd.

SABEL'NIKOV, A. G., AVDEEVA, A. V. & IL'IASHENKO, B. I. 1977. *Escherichia coli* cell competence induced by calcium cations. *Genetika,* 13**,** 1281-1288.

SAMBROOK, J., FRITSCH, E. F. & MANIATIS, T. 1989. *Molecular cloning: a laboratory manual,* New York, Cold Spring Harbor Laboratory Press.

SCHAFER, F. & BUETTNER, G. 2001. Redox environment of the cell as viewed through the redox state of the glutathione disulfide/glutathione couple. *Free Radical Biology and Medicine,* 30, 1191–1212.

SCHÄGGER, H. & VON JAGOW, G. 1987. Tricine-sodium dodecyl sulfate-polyacrylamide gel electrophoresis for the separation of proteins in the range from 1 to 100 kDa. *Analytical Biochemistry,* 166, 368-379.

SEO, H. & LEE, Y. 2010. Characterization of *Deinococcusradiophilus* thioredoxin reductase active with both NADH and NADPH. *Journal of Microbiology,* 48, 637-643.

SIVASHANMUGAM, A., MURRAY, V., CUI, C., ZHANG, Y., WANG, J. & LI, Q. 2009. Practical protocols for production of very high yields of recombinant proteins using *Escherichia coli. Protein Science*, 18, 936-948.

STANTCHEV, T. S., PACIGA, M., LANKFORD, C. R., SCHWARTZKOPFF, F., BRODER, C.C. & CLOUSE, K.A. 2012. Cell-type specific requirements for thiol/disulfide exchange during HIV-1 entry and infection. *Retrovirology*, 9, 97.

STUDIER, F. W. 2005. Protein production by auto-induction in high-density shaking cultures. *Protein Expression and Purification,* 41, 207-234.

TOLEDANO, M., KUMAR, C., LE MOAN, N., SPECTOR, D. & TACNET, F. 2007. The system biology of thiol redox system in *Escherichia coli* and yeast: Differential functions in oxidative stress, iron metabolism and DNA synthesis. *FEBS Letters,* 581, 3598–3607.

TROTTER, E. W. & GRANT, C. M. 2002. Thioredoxins are required for protection against a reductive stress in the yeast *Saccharomyces cerevisiae*. *Molecular Microbiology,* 46, 869-878.

TUROCZI, T., CHANG, V. W., ENGELMAN, R. M., MAULIK, N., HO, Y. S. & DAS, D. K. 2003. Thioredoxin redox signaling in the ischemic heart: an insight with transgenic mice overexpressing thioredoxin-1. *Journal of Molecular and Cellular Cardiology*, 35, 695–704.

VAN LAER, A., DALLALIO, G., MCKENZIE, S. & MEANS R. T. J. 2002. Thioredoxin and protein nitro-tyrosine in bone marrow supernatant from patients with human immunodeficiency virus infection. *Journal of Investigative Medicine,* 50, 10–18.

WANG, Y., ZHANG, X., LIU, Q., AI, C., MO, H. & ZENG, J. 2009. Expression, Purification and Molecular Structure Modeling of Thioredoxin (Trx) and Thioredoxin Reductase (TrxR) from *Acidithiobacillus ferrooxidans*. *Current Microbiology,* 59, 35–41.

WHEELER, G. L. & GRANT, C. M. 2004. Regulation of redox homeostasis in the yeast Saccharomyces cerevisiae. *Physiologia Plantarum,* 120, 12-20.

WILLIAMS, C. 1992. *Chemistry and Biochemistry of Flavoenzymes,* Boca Raton, CRC Press.

WILLIAMS, C., ZANETTI, G., ARSCOTT, L. & MC ALLISTER, J. 1967. Lipoamide Dehydrogenase, Glutathione Reductase, Thioredoxin Reductase and Thioredoxin. *Journal of Biological Chemistry,* 242, 5226-5231.

WILLIAMS, CHJ. 1976. *Flavin-Containing Dehydrogenases*. New York, Academic Press.

WOOF, J. & BURTON, D. 2004. Human antibody-Fc receptor interactions illuminated by crystal structures. *Nature Reviews Immunology,* 4, 89–99.

XU, J., LI, T., WU, H. & XU, T. 2012. Role of thioredoxin in lung disease. *Pulmonary Pharmacology & Therapeutics,* 25, 154-162.

YAMAZAKI, D., MOTOHASHI, K., KASAMA, T., HARA, Y. & HISABORI, T. 2004. Target proteins of the cytosolic thioredoxins in *Arabidopsis thaliana*. *Plant Cell Physiology*, 45, 18–27.

YOSHIHARU, I., WATARU, N., YOKO, T., TAKUMI, O., SHOGO, T., ATSUSHI, K., YOSHIFUMI, K., HIROSHI, M., KAZUO, M., YOSHINORI, W., SHINGO, I. & JUNJI, Y. 2007. Efficient Extraction of Thioreodoxin from *Saccharomyces cerevisiae* by Ethanol. *Applied and Environmental Microbiology,* 73, 1672-1675.

YOSHIOKA, J., SCHREITER, E. & LEE, R. 2006. Role of thioredoxin in cell growth through interactions with signalling molecules. *Antioxidants and Redox Signalling,* 8, 2143–2151.

ZHANG, Y., BAO, R., ZHOU, C. Z. & CHEN, Y. 2008. Expression, purification, crystallization and preliminary X-ray diffraction analysis of thioredoxin Trx1 from *Saccharomyces cerevisiae*. *Acta Crystallographica Section F: Structural Biology and Crystallization Communications,* 64 323-325.

ZHANG, Z., BAO, R., ZHANG, Y., YU, J., ZHOU, C.Z. & CHEN, Y. 2009. Crystal structure of *Saccharomyces cerevisiae* cytoplasmic thioredoxin reductase Trr1 reveals

the structural basis for species-specific recognition of thioredoxin. *Biochimica et Biophysica Acta (BBA) - Proteins and Proteomics,* 1794, 124-128.

Appendix 1

FIX: NADPH NADP InSH InSS IgYSS IgYSH

R1: NADPH + TrxSS = NADP + TrxSH

(kcat1*TR*(NADPH/Knadph)*(TrxSS/K1trxss))/((1+NADPH/Knadph)*(1+TrxSS/K1trxss))

R2: TrxSH + InSS = TrxSS + InSH

k2*TrxSH*InSS

R3: TrxSH + IgYSS = TrxSS + IgYSH

k3*TrxSH*IgYSS

#Species (μM)

NADPH = 400

NADP = 4

InSH = 10

InSS = 2

TrxSH = 1.5

TrxSS = 1.5

IgYSS = 10

IgYSH = 2

Rate parameters

kcat1 = 43.7 s^{-1}

TR = 0.1 μM

Knadph = 1.2 μM

K1trxss = 2.8 μM

k2 = 1

k3 = 1